Article

Technical and Economic Evaluation of CO_2 Capture and Reinjection Process in the CO_2 EOR and Storage Project of Xinjiang Oilfield

Liang Zhang [1,2,*], **Songhe Geng** [1,2], **Linchao Yang** [1,2], **Yongmao Hao** [1,2], **Hongbin Yang** [1,2], **Zhengmiao Dong** [3] **and Xian Shi** [1]

1   School of Petroleum Engineering, China University of Petroleum (East China), Qingdao 266580, China; s19020133@s.upc.edu.cn (S.G.); s20020052@s.upc.edu.cn (L.Y.); haoyongmao@163.com (Y.H.); hongbinyang@upc.edu.cn (H.Y.); 20170003@upc.edu.cn (X.S.)
2   Key Laboratory of Unconventional Oil & Gas Development, China University of Petroleum (East China), Ministry of Education, Qingdao 266580, China
3   Institute of Engineering and Technology, Xinjiang Oilfield Company, Karamay 834000, China; dzm-dm@petrochina.com.cn
*   Correspondence: zhlupc@upc.edu.cn

Abstract: CO_2 capture and reinjection process (CCRP) can reduce the used CO_2 amount and improve the CO_2 storage efficiency in CO_2 EOR projects. To select the best CCRP is an important aspect. Based on the involved equipment units of the CCRP, a novel techno-economic model of CCRP for produced gas in CO_2 EOR and storage project was established. Five kinds of CO_2 capture processes are covered, including the chemical absorption using amine solution (MDEA), pressure swing adsorption (PSA), low-temperature fractionation (LTF), membrane separation (MS), and direct reinjection mixed with purchased CO_2 (DRM). The evaluation indicators of CCRP such as the cost, energy consumption, and CO_2 capture efficiency and purity can be calculated. Taking the pilot project of CO_2 EOR and storage in XinJiang oilfield China as an example, a sensitivity evaluation of CCRP was conducted based on the assumed gas production scale and the predicted yearly gas production. Finally, the DRM process was selected as the main CCRP associated with the PSA process as an assistant option. The established model of CCRP can be a useful tool to optimize the CO_2 recycling process and assess the CO_2 emission reduction performance of the CCUS project.

Keywords: CO_2 EOR and storage; CO_2 capture efficiency; process optimization; economic evaluation; energy consumption

1. Introduction

CO_2 capture and storage (CCS) has been an effective measure to reduce CO_2 emissions into the atmosphere. Injecting CO_2 into oil reservoirs not only can store CO_2 underground, but also can achieve EOR (enhanced oil recovery). However, field experiences show that only less than 50% of the injected CO_2 can be stored if no recycling of the produced CO_2 is considered. A CO_2 capture and reinjection process (CCRP) should be taken to reduce the purchased CO_2 and increase the CO_2 storage efficiency [1]. In the United States and Canada, there have been a large number of CO_2 EOR and storage projects, such as the projects in Weyburn, Rangely, and Kelly-Snyder oil fields [2]. These projects have extensive sources of CO_2, which are captured from natural gas reservoirs or coal gasification plants, transported, and injected in a supercritical state on a large scale. In the earlier days, there were cases using membrane separation (MS) and chemical absorption (CA) methods to capture the CO_2 produced in wells [3–6]. At present, direct reinjection mixed with the necessary pure CO_2 (DRM) to improve the purity of injected gas is commonly adopted especially in the mid-late stage of the CO_2 EOR and storage project [7]. In China, some CO_2 EOR projects have also been conducted, but most of them are on a small scale using

liquid CO_2 purchased from chemical plants [8,9]. Pressure swing adsorption (PSA) and low-temperature fractionation (LTF) processes are often used to capture CO_2 for recycling. In recent years, as more and more natural CO_2 gas reservoirs are discovered in China, the injection scale of CO_2 in oil reservoirs has increased gradually [10–12]. How to optimize a feasible CCRP is becoming more and more important, especially in the context that China is trying to be carbon neutral in the future [13].

At present, many studies have been carried out in the design of CO_2 capture and reinjection. Kwak et al. designed CO_2 recovery plants for EOR application. Four types of CO_2 recovery processes were assessed and a combination of amine, Selexol, and distillation processes were suggested for CO_2 separation [14]. Zhou researched the CA-MDEA (chemical absorption-methyldiethanolamine), LTF, and MS processes to separate CO_2 from the produced gas in the CO_2 EOR project in the Shengli oilfield, and the influences of different operating parameters on the system energy consumption were analyzed [15]. These design works are simulated by commercial softwares, such as Aspen Plus and Unisim, which are suitable for detailed industrial design. For a preliminary assessment, it needs more a convenient and fast-calculation techno-economic model for CO_2 capture. In recent years, Ciferno et al. conducted an economic scoping study for CO_2 capture from flue gas using aqueous ammonia [16]. Kleme et al. developed an overall techno-economic model to compare the CO_2 capture and storage options in coal-fired power plants in the UK, and the cost estimation relationships for the chosen options were calculated [17]. Tuinier et al. evaluated the technical and economic features of a novel cryogenic post-combustion CO_2 capture technology by comparison with the absorption and membrane technology [18]. Huang et al. surveyed the studies about the techno-economic analysis and optimization models for CCS [19]. Zhang assessed the techno-economic aspect of various CCS technologies in coal-fired power plants [20]. Zohrabian et al. calculated the techno-economic indicator of CO_2 capture in integrated hydrogen and powerco-generation system [21]. Zhai et al. evaluated the technical and economic indicators of carbon capture and storage combined with powerco-generation system utilization of deep saline water in the coal chemical project in Ordos, China, and discussed the economic feasibility of the large-scale application of CCS in water-scarce areas [22]. Hu and Zhai performed a systematic economic assessment of the addition of amine-based CCS to coal-fired power plants in China [23]. Liu et al. used the analogy method to establish an economic evaluation model for the entire process of CO_2 capture, utilization, and storage (CCUS), which is more dependent on the relevant economic and technical parameters of the reference target equipment [24]. Decardi-Nelson et al. proposed a novel model of considering the fluctuations in flue gas flow rate to analyze the economic performance in post-combustion CO_2 capture plants [25]. Yun et al. conducted a techno-economic assessment of a novel solvent absorption-based CO_2 capture process for coal-fired power plants [26].

In summary, at present, a lot of techno-economic evaluations and some model studies have been conducted, but most of them are related to CO_2 capture from flue gas and only evaluate the fixed process. Few studies are about the flexible and simple technical and economic evaluation model of CO_2 capture and reinjection in CO_2 EOR and storage project. Compared with the flue gas, the composition of the produced gas in CO_2 flooding is quite complex, and the evaluation of the reinjection process needs to be further considered. Besides, since the thermal power generation is major in China, the equivalent CO_2 emissions caused by equipment energy consumption in CCRP cannot be ignored, but this is rarely studied.

In this paper, a novel techno-economic evaluation model of CCRP for produced gas in CO_2 EOR and storage project was established based on the involved equipment units which can flexibly combine into any CCRPs. The evaluation indicators, including the cost, energy consumption, equivalent CO_2 emissions, CO_2 capture efficiency, and purity of CCRP, could be calculated. Then, the pilot project of CO_2 EOR and storage in XinJiang oilfield China was taken as an example to optimize the CCRP, which can verify the feasibility of the model. The results can guide the design of the CO_2 project in XinJiang oilfield.

2. Potential CCRPs in the CO_2 EOR and Storage Project in XinJiang Oilfield

In many oil fields in the world, CO_2 EOR and storage has been already a common technology, but this is still in its infancy in China. In XinJiang oilfield China, the pilot test of CO_2 EOR and storage has been conducted, but the disposal of produced gas in CO_2 flooding needs to be further studied.

XinJiang oilfield is located in the Junggar Basin of China. The blocks 530 and 53D in XinJiang oilfield are the potential sites for CO_2 EOR and storage, which are about 35 km and 20 km away from XinJiang city, respectively, as shown in Figure 1. After a preliminary evaluation, the Kexia group of block 530 was selected as the target reservoir. This reservoir is a sandy conglomerate formation with a buried depth of 2400 m and a thickness of 18.6 m. The average porosity and permeability are 11.40% and 19.20 md, respectively. 79 wells were deployed in an inverted seven-spot pattern with a well spacing of 280 m × 395 m for water flooding. Due to the low permeability, hydraulic fracturing was conducted in wells. At present, there are 49 wells opened with a daily fluid of 253 t, a daily oil of 68 t, a water cut of 75.9%. 66.25×10^4 t oil has been produced, and the current oil recovery degree is 26.72%.
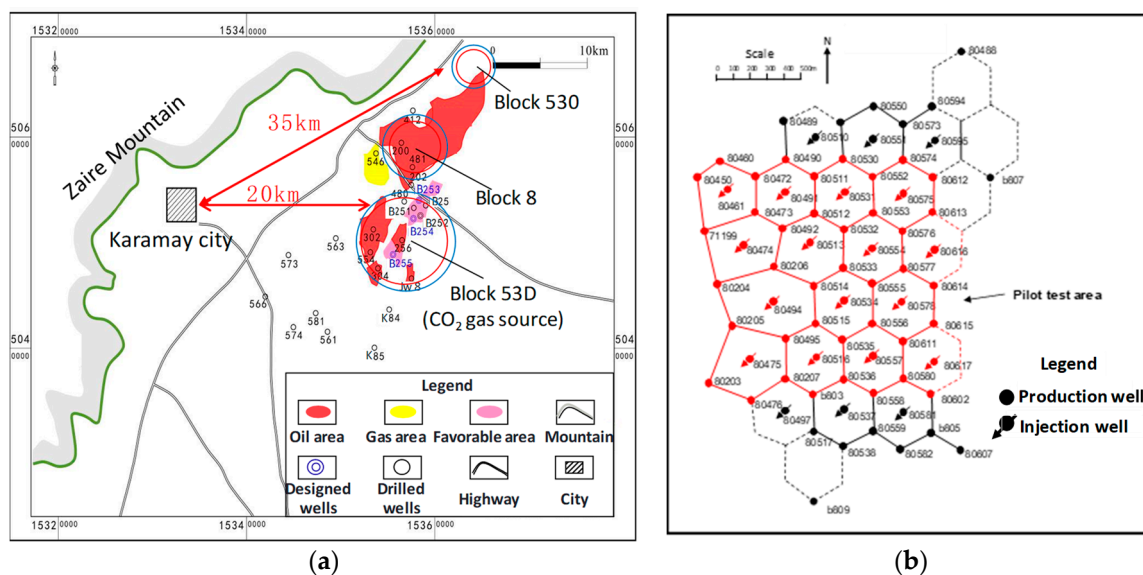

(**a**)   (**b**)

Figure 1. (**a**) The location of block 530 (**b**) Well groups selected in the block 530. The block 530 and well groups selected for CO_2 EOR and storage pilot project.

For the disposal of produced gas in CO_2 flooding in block 530, many methods have been assessed. The schemes of direct reinjection mixed with pure CO_2 (DRM), combustion and flue gas reinjection (CFGR), and CO_2 capture and reinjection were analyzed. The study shows that: (1) the minimum miscible pressure between pure CO_2 and crude oil at the reservoir temperature of 64 °C is 21.25 MPa. Under the original formation pressure of 24 Mpa, if the CO_2 content in the produced gas mixed with necessary pure CO_2 is greater than 90 mol%, it can also achieve miscible flooding; (2) if the produced gas is used for combustion in a heating furnace or a gas turbine, its calorific value should be larger than 584 KJ/mol, and the CO_2 content in the produced gas cannot be higher than 40 mol%, besides, the flue gas produced by combustion can cause severe corrosion and explosion risk during reinjection, hence, the CFGR scheme is unattractive; (3) to purify the CO_2 in the produced gas for reinjection is a commonly used method to dispose of the produced gas, however, four types of CO_2 capture processes have different applicable conditions, thus the CO_2 capture process needs to be further evaluated and optimized according to the CO_2 content and scale of the produced gas.

Therefore, based on the above analysis, five types of CCRPs were designed conceptually for the CO_2 EOR and storage project in block 530, namely the PSA, MS, LTF, CA-MDEA

capture process, and DRM process. Overall, CCRP can be divided into the following three modules: product gas treatment module, carbon capture module, and injection module, and the carbon module is the key difference between the above five types of CCRPs. Hence, taking the PSA capture process as an example (Figure 2a), the detailed capture process is explained: at first, the produced gas is separated from the produced fluid by a three-phase separator, and the solid particles and liquid droplets in the gas are removed through the gas–liquid separator and cyclone separator; then, the produced gas is compressed and pass through the molecular sieve for deep dehydration, and further, the high-purity CO_2 is captured from the produced gas using the PSA system; finally, the captured CO_2 is reinjected back to the oil reservoir at 20 MPa and 40 °C by compressors. For the MS and CA-MDEA processes, they have the similar CCRPs to that of the PSA process except for the CO_2 capture system, while the CO_2 captured in the LTF process should be injected by booster pump at a liquid state under the condition of 20MPa and −20 °C [27–29]. When the DRM process is adopted (Figure 2b), the produced gas can be reinjected directly after being pretreated. If necessary, before reinjection, the produced gas should be mixed with pure CO_2 to reach the required gas amount and CO_2 purity.
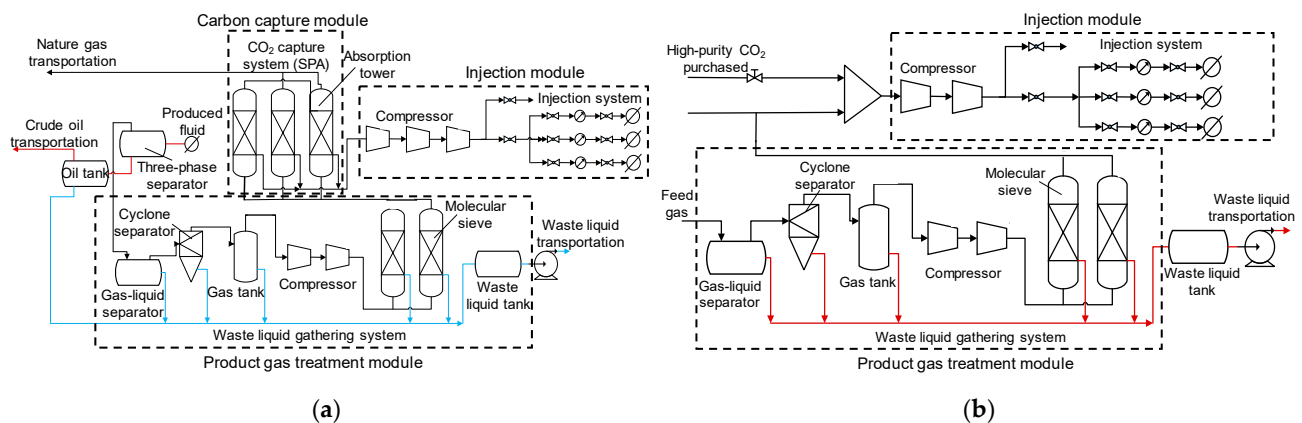

(**a**)

(**b**)

Figure 2. The CCRPs designed in CO_2 EOR and storage project in XinJiang Oilfield. (**a**) Typical CO_2 PSA capture and reinjection process; (**b**) Direct reinjection process with purchased CO_2.

According to the function of each module, some necessary simplifications were carried out to unify the five types of CCRPs into one process for flexible technical and economic evaluation, as shown in Figure 3. In this simplified process, the main equipment units are gas–liquid separator, molecular sieve, compressor, boost pump, and carbon capture module. Among them, the gas–liquid separator and molecular sieve are units for dust removal and dehydration, compressor and boost pump are used to transport and inject liquid or gas CO_2, and carbon capture module is the critical unit for capture CO_2. Since the produced gas is processed on-site, the pipeline is not considered in this simplified process. The simplified process corresponding to each CCRP is shown in Table 1.
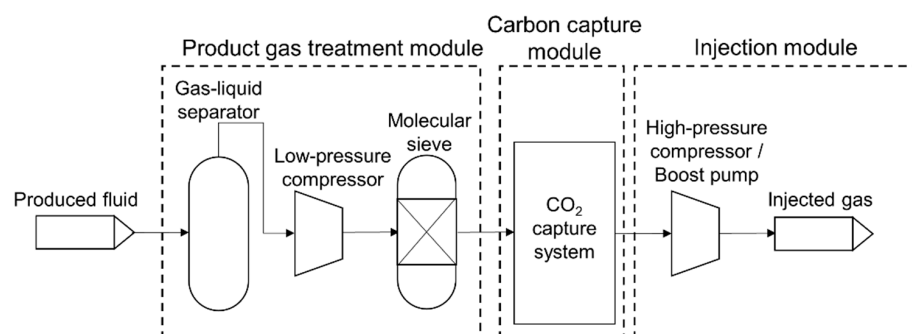

Figure 3. Main equipment units involved in the simplified CCRP.

Table 1. Main equipment units involved in the five types of CCRPs.

The Types of CCRPs	The 6 Main Equipment Units
SPA	Produced gas (0.5 MPa, 20 1 °C) → gas–liquid separator → low-pressure compressor → molecular sieve → SPA system → high-pressure compressor →reinjected gas (20 MPa, 40 °C)
MS	Produced gas (0.5 MPa, 20 °C) → gas–liquid separator → low-pressure compressor → molecular sieve → MS system → high-pressure compressor →reinjected gas (20 MPa, 40 °C)
LTF	Produced gas (0.5 MPa, 20 °C) → gas–liquid separator → low-pressure compressor → molecular sieve → LTF system → liquid CO_2 storage tank → boost pump→ reinjected gas (20 MPa, −20 °C)
CA-MDEA	Produced gas (0.5 MPa, 20 °C) → gas–liquid separator → low-pressure compressor → molecular sieve → CA-MDEA → high-pressure compressor →reinjected gas (20 MPa, 40 °C)
DRM	Produced gas (0.5 MPa, 20 °C) → gas–liquid separator → low-pressure compressor → molecular sieve → high-pressure compressor →reinjected gas (20 MPa, 40 °C)

3. Establishment of Technical and Economic Evaluation Model of CCRP

To be used to flexibly calculate the process parameters, cost, energy consumption, and CO_2 capture efficiency for different CCRPs, the indicator calculation model for each possible involved equipment unit was established. Based on the equipment units, the indicators of the entire CCRP can be obtained.

3.1. Calculation Method of Capital Cost

Based on the main technical parameters of each equipment unit, the capital cost and the power can be estimated [30]. The main power/energy consumption units in CCRP include compressor, booster pump, and carbon capture module. For the no energy consumption units such as the gas–liquid separator and molecular sieve, their capital costs can be estimated by the analogy method.

3.1.1. Gas–Liquid Separator and Molecular Sieve

In CCRPs, both gas–liquid separator and molecular sieve have extremely low energy consumption in the process of dust removal and dehydration for produced gas, thus the analogy method is used to obtain their capital costs. According to the scale of the disposal gas, the capital cost can be calculated based on the following empirical formula [31]:

$$C_{sep} = \alpha_{sep1} \times \left(\frac{M_{train}}{10^5} \right)^{\alpha_{sep2}} \tag{1}$$

$$C_{mol} = \alpha_{mol1} \times \left(\frac{M_{train}}{10^5} \right)^{\alpha_{mol2}} \tag{2}$$

where C_{sep} is the capital cost of gas–liquid separator, US$; M_{train} is the mass flow rate of disposal gas, t/d; C_{mol} is the capital cost of molecular sieve, US$; α_{sep1} and α_{sep2} are the cost coefficients of gas–liquid separator, taking 11 US$ and 0.6, respectively; α_{mol1} and α_{mol2} are the cost coefficients of molecular sieve cost, taking 19 US$ and 0.6, respectively. The above cost coefficients are obtained based on the capital cost of the gas–liquid separator and molecular sieve in the Chinese oilfield [13,32,33].

3.1.2. Compressor

In oil fields, compressors and booster pumps are the most used equipment to increase fluid pressure. Compressors are suitable for CO_2 in gas and supercritical state, while pumps

are suitable for liquid CO_2 or high-dense CO_2. For the capital cost of compressors, it can be estimated according to the CO_2 flow rate and the ratio of gas pressures at the outlet and inlet of the compressor. For the estimation of the compressor power, the physical properties of CO_2 gas and the multi-stage compression process with the optimal compression ratio for each stage should be considered.

(1) For the capital cost of the compressor [34],

$$C_{comp} = m_{train}N_{train}\left[\left(\alpha_{comp1}(m_{train})^{\alpha_{comp2}} + \alpha_{comp3}(m_{train})^{\alpha_{comp4}}\ln\left(\frac{P_{out-comp}}{P_{in-comp}}\right)\right)\right] \quad (3)$$

$$m_{train} = \frac{(1000 \times m_{CO_2})}{(24 \times 3600 \times N_{train})} \quad (4)$$

where C_{comp} is the total capital cost of compressor, US\$; m_{train} is the mass flow rate of CO_2 gas in each compressor unit, kg/s; N_{train} is the number of parallel compressors, dimensionless; m_{CO_2} is the CO_2 mass flow rate, t/d; $P_{in\text{-}comp}$ is the inlet pressure of compressor, MPa; $P_{out\text{-}comp}$ is the outlet pressure of compressor, MPa; α_{comp1}, α_{comp2}, α_{comp3} and α_{comp4} are the cost coefficients of compressor, taking 0.12×10^6 US\$·kg^{-1}·s, -0.71, 1.32×10^6 US\$·kg^{-1}·s and -0.60, respectively, which are converted from € into US\$ at the current exchange rate [34].

(2) For the compressor power [35],

$$W_{comp} = \left(\frac{1000}{24 \times 3600}\right)\left(\frac{m_{CO_2}Z_sRT_{in-comp}}{M_{CO_2gas}\eta_{comp}}\right)\left(\frac{k_s}{k_s-1}\right)\left[(CR)^{\frac{k_s-1}{k_s}} - 1\right] \quad (5)$$

$$CR = \left(\frac{P_{out-comp}}{P_{in-comp}}\right)^{\frac{1}{N_{stage}}} \quad (6)$$

where W_{comp} is the compressor power, kW; Z_s is the average compression factor of CO_2 at each stage, dimensionless; $T_{in\text{-}comp}$ is the inlet temperature of compressor, K; R is the universal gas constant, 8.314 kJ/(kmol·K); M_{CO_2gas} is the molar mass of CO_2 gas, if the CO_2 purity of gas is 100%, M_{CO_2gas} = 44.01 kg/kmol; η_{comp} is the compressor efficiency, 0.75 is often used; k_s is the average heat capacity ratio of CO_2 at each stage, 1.391 is often used; CR is the optimal compression ratio, 2.4–3.0 is often used; N_{stage} is the number of compression stages. The maximum power of a single compressor was assumed to be 40MW. If the required compression power is greater than 40 MW, several parallel compressors will be used, and the N_{train} is $W_{comp}/40$.

3.1.3. Booster Pump

In the CCRP, after being purified and liquefied, the liquid CO_2 can be transported and injected into the subsequent processes using booster pumps. The capital cost of booster pumps mainly depends on the pump power, while the pump power is selected based on the flow rate and pressures of CO_2 at the inlet and outlet of the pump [36].

(1) For the capital cost of the pump,

$$C_{pump} = \alpha_{pump1} \times \left(\frac{W_{pump}}{1000}\right) + \alpha_{pump2} \quad (7)$$

(2) For the pump power,

$$W_{pump} = \left(\frac{1000 \times 10}{24 \times 36}\right)\left[\frac{m_{CO_2}(P_{out-pump} - P_{in-pump})}{\rho_{l-CO_2}\eta_{pump}}\right] \quad (8)$$

where C_{pump} is the capital cost of booster pump, US\$; W_{pump} is the booster pump power, kW; $P_{out-pump}$ is the outlet pressure of booster pump, MPa; $P_{in-pump}$ is the inlet pressure of booster pump, MPa; ρ_{l-CO_2} is the density of liquid CO_2, 1177 kg/m^3; η_{pump} is the efficiency of booster pump, 0.75 was assumed; α_{pump1} and α_{pump2} are the cost coefficients of pump, taking 1.14×10^6 US\$·W^{-1} and 0.07×10^6 US\$, respectively.

3.1.4. Carbon Capture Module

The commonly used CO_2 capture modules include pressure swing adsorption (PSA), membrane separation (MS), low-temperature fractionation (LTF), and chemical absorption (CA-MDEA).

(1) Pressure swing adsorption (PSA)

In the PSA module, according to the difference of adsorption characteristics of different kinds of gases in physical adsorbent with pressure, specific gas (e.g., CO_2) will be absorbed and desorbed through periodic pressure changes to achieve the purpose of gas separation and purification [37]. The capital cost of the PSA CO_2 capture module is mainly composed of three parts: the capital cost of adsorption towers, the purchase cost of adsorbent, and the capital cost of the compressor.

First, the mass of CO_2 adsorbent for PSA can be calculated based on the gas production, CO_2 content in produced gas, and the adsorption capacity of the adsorbent [38].

$$W_{PSA-ad} = Q_{PSA-g} \times t_{PSA-ad} \times y_{PSA-CO_2} / \Delta q_{PSA} \times n_{PSA-bed} \tag{9}$$

where W_{PSA-ad} is the mass of adsorbent in PSA module, kg; Q_{PSA-g} is the flow rate of the feed gas in the adsorption tower of PSA module, m^3/s; t_{PSA-ad} is the adsorption time of single bed operation of the tower in PSA module, s; y_{PSA-CO_2} is the CO_2 mole fraction of the feed gas in PSA module, dimensionless; Δq_{PSA} is the adsorption capacity in PSA module which depends on the adsorbent, for silica 0.35–0.50 kg/kg is taken, for activated carbon 0.40–0.50 kg/kg is taken, and for molecular sieves, 0.22–0.26 kg/kg is taken [39]; $n_{PSA-bed}$ is the number of beds for continuous adsorption in a single tower in PSA module, dimensionless.

Then, according to the mass of the adsorbent and the design requirements of the adsorption tower, the height, diameter, and number of the adsorption towers can be calculated [40].

$$H_{PSA} = \frac{W_{PSA-ad}}{n_{PSA-tower}\rho_{PSA-ad}} \frac{v_{PSA-g}}{Q_{PSA-g}} \tag{10}$$

$$D_{PSA} = H_{PSA}/(5 \sim 8) \tag{11}$$

$$n_{PSA-tower} = \frac{W_{PSA-ad}}{\rho_{PSA-ad}} \frac{4}{3.14 D_{PSA}^2 H_{PSA}} \tag{12}$$

where H_{PSA} is the height of the tower in PSA module, m; $n_{PSA-tower}$ is the number of towers in PSA module dimensionless; ρ_{PSA-ad} is the adsorbent density in PSA module, for silica 0.70–0.82 kg/m^3 is taken, for activated carbon 0.45–0.50 kg/m^3 is taken, and for molecular sieves, 0.61–0.67 kg/m^3 is taken; v_{PSA-g} is the gas flow speed in the tower, 0.05 m/s was assumed according to common design of CO_2 absorption tower [41]; D_{PSA} is the diameter of the tower in PSA module, m.

Finally, through the unit height capital cost of the tower and the sizes of the tower, the capital cost of adsorption towers can be obtained [41].

$$C_{PSA-tower} = C_{PSA-pc} \times H_{PSA} \times n_{PSA-tower} \tag{13}$$

$$\log C_{PSA-pc} = \alpha_{PSA1} \log D_{PSA} + \alpha_{PSA2} \tag{14}$$

where $C_{PSA-tower}$ is the capital cost of towers in PSA module, US\$; C_{PSA-pc} is the unit height capital cost of the tower in PSA module, US\$/m; α_{PSA1} and α_{PSA2} are the cost coefficients of PSA module, taking 1.34 and 4.27, respectively.

CO_2 adsorbent with excellent adsorption and desorption performance should be selected for PSA. The commonly used adsorbents can be classified into carbon-based adsorption materials (e.g., activated carbon) and zeolite adsorption materials (e.g., 13X molecular sieve). The 13X is often used because of its large pore volume, high adsorption capacity, and high separation coefficient. Hence, the purchase cost of adsorbent can be determined as follows [39]:

$$C_{PSA-ad} = P_{PSA-ad} \times W_{PSA-ad} \tag{15}$$

where C_{PSA-ad} is the purchase cost of adsorbent in PSA module, US\$; P_{PSA-ad} is the unit cost of adsorbent, for silica 1.58 US\$/kg is taken, for activated carbon 0.47 US\$/kg is taken, and for molecular sieves, 1.58 US\$/kg is taken.

Based on the above, the capital cost of the PSA module can be calculated.

$$C_{PSA} = C_{PSA-tower} + C_{PSA-ad} + C_{comp} \tag{16}$$

where C_{PSA} is the capital cost of the PSA module, US\$.

The power consumption in the PSA module mainly occurs when the feed gas is compressed to meet the adsorption pressure in towers, thus the power of the PSA module is equal to the power of the compressor.

$$W_{PSA} = W_{comp} \tag{17}$$

where W_{PSA} is the power of the PSA module, kW.

It should be noted that if the pressure of feed gas is high enough which can meet the requirement of adsorption pressure in towers, the compression process can be neglected in the PSA module, no power consumption is considered.

(2) Membrane separation (MS)

In the MS module, the penetrability difference of each component in feed gas through the polymer membrane under a certain pressure is used to separate the CO_2 from the hydrocarbon gas. The capital cost of the MS module mainly comes from the compressor and the MS device [42]. The capital cost of the MS device, which consists of membrane material and frame, is determined by the film type and film property. The components in feed gas can be divided into the high-speed group and the low-speed group according to their difference in permeation rate through the membrane. Hence, the film area can be estimated as follows [5]:

$$A_m = \frac{Q_{MS-p} Y_{MS-1}}{\dfrac{R_{MS-f}\left(P_{MS-2}\left(\dfrac{Y_{MS-F} - Y_{MS-R}}{\ln\left(\frac{Y_{MS-F}}{Y_{MS-R}}\right)}\right) - P_{MS-1} Y_{MS-1}\right)}{100}} \tag{18}$$

where A_m is the film area in MS module, m^2; Y_{MS-F} is the mole fraction of high-speed group (CO_2) in feed gas in MS module, dimensionless; Y_{MS-R} is the mole fraction of the high-speed group in the nonpenetrating gas in MS module, dimensionless; Y_{MS-1} is the mole fraction of the high-speed group in the permeation gas in MS module, dimensionless; Q_{MS-P} is the flow rate of permeation gas in MS module, kmol/s; R_{MS-f} is the weighted average permeation velocity of the high-speed group in MS module, m/s; P_{MS-1} is the total pressure on the low-pressure side of the membrane in MS module, bar; and P_{MS-2} is the total pressure on the high-pressure side of the membrane in MS module, bar.

The membranes used for CO_2 separation are mainly made of high molecular polymers, such as polydimethylsiloxane, cellulose acetate, polyimide, polysulfone, polycarbonate, etc. Due to the high permeation speed and excellent separation effect, polyimide has been widely used in China, and its hollow fiber membrane module has a low cost, high loading density, and adaptability to high pressure, which is often selected. [43] Hence, based on the

film area and type, the capital cost of MS device can be estimated using the equations as follows [42]:

$$C_M = I_m + I_{mf} \tag{19}$$

$$I_m = A_m K_m \tag{20}$$

$$I_{mf} = \left(\frac{A_m}{\alpha_{m1}}\right)^{\alpha_{m2}} K_{mf} \tag{21}$$

where C_M is the capital cost of MS device, US\$; I_m is the cost of membrane material in MS device, US\$; I_{mf} is the cost of membrane frame in MS device, US\$; K_m is the membrane material cost of unit film area, 4.73–18.93 US\$/m^2 for hollow fiber membrane module; K_{mf} is the membrane frame cost of unit film area, 315.46 US\$/m^2, the above MS device costs of unit film area are from the price survey in China; and α_{m1} and α_{m2} are the cost coefficients of MS module, taking 2000 and 0.7, respectively.

Hence, based on the above, the capital cost of the MS carbon capture module can be obtained.

$$C_{MS} = C_M + C_{comp} \tag{22}$$

where C_{MS} is the capital cost of MS module, US\$.

Similarly, the power consumption of the MS module mainly occurs when the feed gas is needed to be compressed to form a high-enough permeation pressure difference on both sides of the membrane, so the power of the MS module is equal to the power of the compressor.

$$W_{MS} = W_{comp} \tag{23}$$

where W_{MS} is the power of the MS module, kW.

(3) Low-temperature fractionation (LTF)

In the LTF module, the separation of CO_2 from feed gas is realized based on the difference in boiling temperature of each component in the feed gas. The pressurization effect of the compressor and the cooling effect of the heat exchanger is utilized to achieve the gas liquefaction. For the heat exchanger, after the structure is determined, the technical and economic model of the heat exchanger can be established based on the heat exchange area [15]. The heat exchange area can be determined by the parameters in the operating environment of the heat exchanger. When the heat exchanger recovers waste heat, it also needs to consume some power to overcome the flowing resistance of fluid passing through the heat exchanger and the cooler. This power consumption is the operating cost of the equipment [44].

$$C_{hx} = \alpha_{hx1} + \alpha_{hx2} A_{hx-p}^{\alpha_{hx3}} \tag{24}$$

$$A_{hx-p} = \alpha_{hx4} \frac{Q_{hx}}{K_{hc} \Delta T_m} \tag{25}$$

$$Q_{hx} = m_{hf} C_p \Delta t_{hx} \tag{26}$$

$$\Delta T_m = \frac{(T_{HI} - T_{CO}) - (T_{HO} - T_{CI})}{\ln \frac{T_{HI} - T_{CO}}{T_{HO} - T_{CI}}} \tag{27}$$

$$W_{hx} = A_{hx-p} \cdot K_{hc} \cdot \Delta t_{hx} / 1000 \tag{28}$$

where C_{hx} is the capital cost of the heat exchanger, US\$; A_{hx-p} is the actual heat exchange area in heat exchanger, m^2; α_{hx1}, α_{hx2} and α_{hx3} are the cost coefficients of heat exchanger, taking 9.41×10^4 US\$, 1.13×10^3 US\$ and 0.98, respectively; α_{hx4} is the coefficients obtained by unit conversion, 0.28; Q_{hx} is the heat flow in heat exchanger, kJ/h; m_{hf} is the mass flow rate of hot fluid in heat exchanger, kg/h; C_p is the specific heat capacity of fluid in heat exchanger in heat exchanger, kJ·kg^{-1}·°C^{-1}; Δt_{hx} is the temperature change of hot fluid in heat exchanger, °C; ΔT_m is the logarithmic mean temperature changes of heat exchanger, °C; T_{HI} is the hot fluid temperature at the inlet of the heat exchanger, °C; T_{HO} is the hot fluid temperature at the outlet of the heat exchange, °C; T_{CI} is the cold fluid

temperature at the inlet of the heat exchanger, °C; T_{CO} is the cold fluid temperature at the outlet of the heat exchanger, °C; W_{hx} is the power of heat exchanger, kW; and K_{hc} is the heat transfer coefficient between the hot fluid and the cold fluid, taking 1134 W/(m^2·°C) (between liquid-phase fluids) or 279 W/(m^2·°C) (between gas-phase fluids).

Hence, the capital cost of the LTF module is mainly composed of the capital costs of the compressor and heat exchanger [45]. Similarly, the power of LTF covers the powers of the compressor and heat exchanger.

$$C_{LTF} = C_{comp} + C_{hx} \tag{29}$$

$$W_{LTF} = W_{comp} + W_{hx} \tag{30}$$

where C_{LTF} is the capital cost of LTF module, US\$; W_{LTF} is the power of LTF module, kW.

(4) Chemical absorption (CA-MDEA)

In the CA module, CO_2 is captured from the feed gas by a chemical reaction between alkaline solution and CO_2. CO_2 is absorbed by the alkaline solution at a low temperature and desorbed at a high temperature. The capital cost of the chemical absorption module includes the capital costs of solvent towers, booster pumps, heat exchangers, and the purchase cost of chemical absorption solution [14]. MDEA (methyldiethanolamine) is the often used solvent for CO_2 chemical absorption. Hence, the MDEA is taken as a typical example to establish the capital cost calculation model of CA.

The solvent towers mainly include the absorption tower and the desorption tower. For the absorption tower, firstly, the diameter of the tower can be determined according to feed gas flow; and then, the height of the tower can be estimated according to the tower diameter and CO_2 absorption capacity of MDEA; finally, based on the cost of unit height tower, the capital cost of absorption tower can be obtained [40,46–48].

$$D_{CA-ab} = \sqrt{\frac{4V_{CA-ab}}{3600\pi v_{CA-ab}}} \tag{31}$$

$$H_{CA-ab} = \frac{m_{CA-CO_2}/M_{CO_2gas}}{K_{Ga}A_{CA-t}\Delta P_{CA-m}} ln\left(\frac{Y_{CO_2-inab}}{Y_{CO_2-outab}}\right) \tag{32}$$

$$A_{CA-t} = \frac{\pi D_{CA-ab}{}^2}{4} \tag{33}$$

$$\log C_{CA-ab} = \alpha_{ab1} \log D_{CA-ab} + \alpha_{ab2} \tag{34}$$

$$C_{CA-abt} = C_{CA-ab} \times H_{CA-ab} \tag{35}$$

where D_{CA-ab} is the diameter of absorption tower in CA module, m; V_{CA-ab} is the flow rate of feed gas in the absorption tower in the CA module, m^3/h; v_{CA-ab} is the gas flow velocity in the adsorption tower which should make sure that the CO_2 in feed gas can fully combine with the MDEA solution, 0.722 m/s was used according to the common design for the chemical absorption tower [41]; H_{CA-ab} is the cumulative height of absorption towers in the CA module, m; m_{CA-CO_2} is the mass flow rate of CO_2 gas in CA module, kg/h; K_{Ga} is the mass transfer coefficient, 20 kmol/(m^3·h·atm) was taken from the calculation process of Zhang [46]; Y_{CO_2-inab} is the CO_2 content of inlet gas in the absorption tower, g/m^3; $Y_{CO_2-outab}$ is the CO_2 content of outlet gas in the absorption tower, g/m^3; A_{CA-t} is the cross-section area of absorption tower in CA module, m^2; ΔP_{CA-m} is the driving pressure difference, the default value is 0.026 atm at the oilfield site; C_{CA-ab} is the cost of the unit height tower in the CA module, US\$/m; C_{CA-abt} is the capital cost of the absorption tower in the CA module, US\$; and α_{ab1} and α_{ab2} are the cost coefficients of the absorption tower in the CA module, taking 1.34 and 4.27, respectively, based on the data from the Chinese oilfield [12,32].

Similarly, the capital cost of desorption tower can be calculated using the following formulas [46,47]:

$$D_{CA-de} = \sqrt{\frac{4V_{CA-de}}{3600\pi v_{CA-de}}} \tag{36}$$

$$N_{CA-t} = m_{CA-CO_2}/M_{CO_2 gas}/\alpha_{de1} \tag{37}$$

$$\log C_{CA-de} = \alpha_{de2}(\log D_{CA-de})^2 + \alpha_{de3}\log D_{CA-de} + \alpha_{de4} \tag{38}$$

$$C_{CA-det} = C_{CA-de} \times N_{CA-t} \tag{39}$$

where D_{CA-de} is the diameter of the desorption tower in CA module, m; V_{CA-de} is the flow rate of feed gas in the desorption tower in the CA module, m^3/h; v_{CA-de} is the gas flow velocity in the desorption tower which should make sure that the CO_2 can be effectively separated from the MDEA solution, 0.91 m/s was used according to the common design for chemical absorption tower [41]; N_{CA-t} is the total number of theoretical plates in the desorption tower in the CA module, dimensionless; C_{CA-de} is the tower cost of a single plate of the desorption towers in the CA module, US\$; α_{de1} is the mole flow rate which can be supported by one plate based on the common design of the desorption tower, 6.96 kmol/h is used [41]; α_{de2}, α_{de3} and α_{de4} are the cost coefficients of the desorption tower in the CA module, taking 0.56, 1.06 and 3.89, respectively, based on the data from Chinese oilfield [12,32]; and C_{CA-det} is the capital cost of the desorption tower in the CA module, US\$.

The purchase cost of the MDEA solution can be calculated according to the required circulation amount of MDEA solution, which can be estimated based on the CO_2 absorption capacity of MDEA [48].

$$M_{MDEA} = \alpha_{MDEA} \times m_{CA-CO_2}/M_{CO_2 gas} \tag{40}$$

$$C_s = M_{MDEA} \times C_{us} \tag{41}$$

where M_{MDEA} is the required circulation amount of the MDEA solution, t; C_s is the purchase cost of MEDA solution, US\$; C_{us} is the unit cost of the MEDA solution, 2176.66 US\$/t was referenced; and α_{MDEA} is the circulation amount of the MDEA solution which can be used to absorb the unit mole flow rate of CO_2 gas, based on the reaction mechanism between DMEA and CO_2 and the common design of the CO_2 absorption tower, 0.73 $t \cdot kmol^{-1} \cdot h$, is taken [49].

Based on the above analysis, the capital cost of the MEDA carbon capture module can be obtained.

$$C_{CA} = C_{CA-abt} + C_{CA-det} + C_s + C_{pump} + C_{hx} \tag{42}$$

Then, the power of the MEDA module can be calculated as follows.

$$W_{CA} = W_{pump} + W_{hx} \tag{43}$$

where C_{CA} is the capital cost of CA module, US\$; W_{CA} is the power of CA module, kW.

3.2. Calculation Method of Running Cost

The running cost of each equipment unit mainly includes the maintenance cost and operating cost. Maintenance cost refers to the fees paid to maintain or restore the technical performance of the equipment. Operating cost is mainly the energy cost of the equipment, which is generally the electric charge calculated according to the equipment power. Hence, the running cost of the entire process can be obtained as follows.

$$O\&M_{annual} = \sum(C_{unit} \times M_{factor} + W_{unit} \times 24 \times 365 \times F_{elec}) \tag{44}$$

where $O\&M_{annual}$ is the annual running cost of CCRP, US\$; C_{unit} is the capital cost of equipment unit, US\$; M_{factor} is the ratio of annual maintenance cost to total infrastructure

cost, 0.05 is often used; W_{unit} is the power of equipment unit, kW; F_{elec} is the electricity price, generally 0.08 US\$/kWh is taken in China.

3.3. Calculation Method of CO₂ Capture Parameters

In CCRP, the gas flow rate and CO_2 content will change, especially before and after the carbon capture module. Due to the limit of capture purity, part of CO_2 will be lost in the separated hydrocarbon gas. Moreover, China's power generation is still dominated by thermal power using coal at present, thus the energy consumption of each equipment unit during operation is equivalent to an additional amount of CO_2 emissions. Therefore, the concepts of CO_2 flow, energy consumption equivalent CO_2 emissions, and CO_2 capture efficiency of basic equipment units were proposed.

As shown in Figure 4, taking the CO_2 capture module as an example, the CO_2 flow should satisfy the material balance when the CO_2-contained gas flows through the capture equipment. If the gas flow rate and CO_2 content at the inlet are defined to be $Q_{in\text{-}gas}$ and $x_{in\text{-}CO_2}$, respectively, then the pure CO_2 gas flow rate at the inlet is $Q_{in\text{-}CO_2} = Q_{in\text{-}gas} \times x_{in\text{-}CO_2}$. For the gas flow at the outlet, $Q_{out\text{-}gas}$, it is divided into the CO_2 gas flow $Q_{out\text{-}CO_2gas}$ and the hydrocarbon gas flow $Q_{out\text{-}CH4gas}$; if their CO_2 and hydrocarbon gas purities are $x_{out\text{-}CO_2}$ and $y_{out\text{-}CH4}$, respectively, then the captured pure CO_2 gas flow rate is $Q_{out\text{-}CO_2} = Q_{out\text{-}CO_2gas} \times x_{out\text{-}CO_2}$, and the CO_2 lost in hydrocarbon gas is $Q_{out\text{-}CO_2\text{-}loss} = Q_{out\text{-}CH4gas} \times (1 - y_{out\text{-}CH4})$. Moreover, the additional CO_2 emission released by coal-fired power generation due to energy consumption during capture is $Q_{power\text{-}CO_2}$, then the CO_2 capture efficiency of the capture module can be calculated to be $\eta = (Q_{out\text{-}CO_2} - Q_{power\text{-}CO_2})/Q_{in\text{-}CO_2}$. Similarly, the CO_2 flow variation and CO_2 capture efficiency of other equipment units in CCRP can also be obtained, as shown in Table 2. Based on these equations, the indicators of the entire CCRP can be determined. For the CO_2 capture and reinjection efficiency (CCRE) of the CCRP, it can be calculated based on the total $Q_{power\text{-}CO_2}$, $Q_{out\text{-}CO_2}$, and $Q_{in\text{-}CO_2}$ of the process, or calculated by multiplying the CO_2 capture efficiencies of all units in the process.
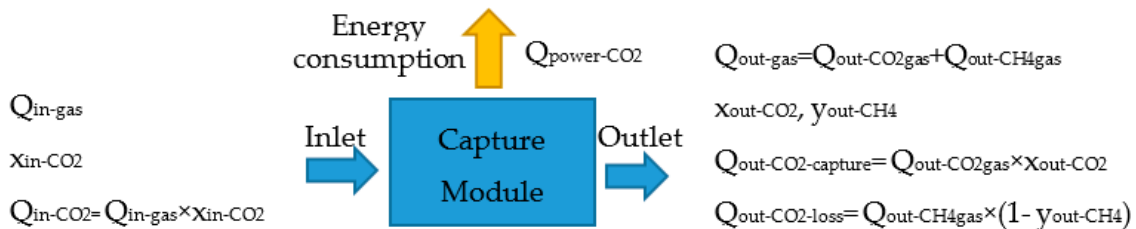

Figure 4. Variation of CO_2 flow through capture module.

Table 2. CO_2 flow variation and CO_2 capture efficiency of each equipment unit in CCRP.

Equipment Units	Gas Flow at the Outlet, m³/d	CO₂ Purity at the Outlet, Fraction	CO₂ Flow at the Outlet, m³/d	Additional CO₂ Emission, m³	CO₂ Capture Efficiency, Fraction
Compressor/Pump	$Q_{out\text{-}gas} = Q_{in\text{-}gas}$	$x_{out\text{-}CO_2} = x_{in\text{-}CO_2}$	$Q_{out\text{-}CO_2} = Q_{out\text{-}gas} \times x_{out\text{-}CO_2}$	$Q_{power\text{-}CO_2}$	$H = (Q_{out\text{-}CO_2} - Q_{power\text{-}CO_2})/Q_{in\text{-}CO_2}$
Carbon Capture Module	$Q_{out\text{-}CO_2gas}$ $Q_{out\text{-}CH4gas}$ $Q_{in\text{-}gas} = Q_{out\text{-}CO_2gas} + Q_{out\text{-}CH4gas}$	$x_{out\text{-}CO_2}$ $y_{out\text{-}CH4}$ $Q_{in\text{-}gas} \times x_{in\text{-}CO_2} = Q_{out\text{-}CO_2gas} \times x_{out\text{-}CO_2} + Q_{out\text{-}CH4gas} \times (1 - y_{out\text{-}CH4})$	$Q_{out\text{-}CO_2} = Q_{out\text{-}CO_2gas} \times x_{out\text{-}CO_2}$	$Q_{power\text{-}CO_2}$	$H = (Q_{out\text{-}CO_2} - Q_{power\text{-}CO_2})/Q_{in\text{-}CO_2}$

For the $Q_{power\text{-}CO_2}$, it can be estimated based on the power of the equipment unit, coal consumption required for unit power generation, and the CO_2 emission per unit coal by burning, as follows [50]:

$$Q_{power-CO_2} = W_{unit} \times t_u \times M_{coal} \times E_{CO_2}/\rho_{CO_2} \tag{45}$$

where $Q_{power-CO_2}$ is the energy consumption equivalent CO_2 emission of equipment unit, Sm^3/d; t_u is the unit time, h; M_{coal} is the coal consumption required for unit power generation, 0.313 kg/kWh was taken; E_{CO_2} is the CO_2 emissions per unit coal by burning, generally 2.6 kg CO_2/kg coal is used; t_u is unit time, taking 24 h; and ρ_{CO_2} is the density of CO_2 gas, taking 1.98 kg/m^3.

For the gas capture purity, we have conducted a sensitivity simulation for different kinds of carbon capture modules using the software Aspen Hysys 2006. The composition of feed gas referred to the associated gas in Block 530 in XinJiang oilfield, which has 84.98% C1, 7.21% C2, 3.04% C3, 1.23% C4, 0.54% C5, 2.60% N_2, and 0.4% CO_2. By mixing CO_2 with the associated gas, feed gases with different CO_2 contents and at different flow rates were input in the simulation models for calculation. The results show that the capture purity of gas is mainly determined by the CO_2 content in the feed gas. Hence, we regressed the relation equations of gas capture purity with CO_2 content in feed gas for usage in our models to calculate the CO_2 flow variation, as shown in Figure 5 and Table 3. It can be seen that as the CO_2 content in feed gas increases, the CO_2 capture purity of PSA, MS, LTF modules gradually increases, while the CO_2 capture purity of the MDEA module is always high. When the CO_2 content in the feed gas is larger than 75 mol%, all the CO_2 capture purities of all capture modules can reach larger than 90 mol%. Overall, the ranking of CO_2 capture purity is MDEA > PSA > MS > LTF. The CO_2 capture purity of the LTF module is the lowest one, because a part of liquefied C2+ can mix into liquid CO_2 and hardly be separated. On the other side, the purity of natural gas ranks in an order of MDEA >LTF> PSA > MS.
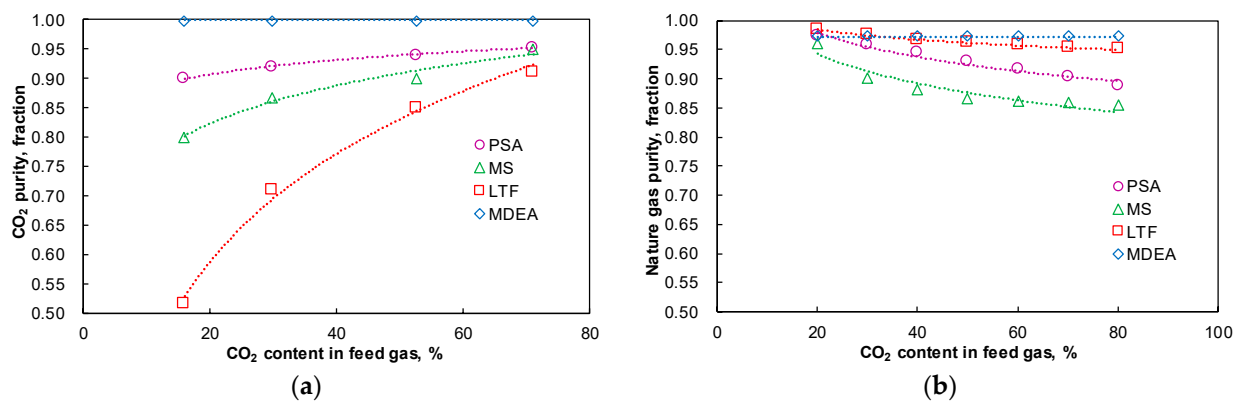

Figure 5. (**a**) CO_2 capture purity, (**b**) hydrocarbon gas capture purityGas capture purity at different CO_2 contents in the feed gas.

Table 3. Regression formulas of gas capture purity for different CO_2 capture modules.

Gas Purity	Capture Type	Regression Formula	Correlation Coefficient R^2
CO$_2$ purity of captured CO$_2$ gas	PSA	$x_{out-CO_2} = 0.036\ln x_{in-CO_2} + 0.8002$	$R^2 = 0.9952$
	MS	$x_{out-CO_2} = 0.094\ln x_{in-CO_2} + 0.5420$	$R^2 = 0.9734$
	LTF	$x_{out-CO_2} = 0.265\ln x_{in-CO_2} - 0.2061$	$R^2 = 0.9934$
	MDEA	$x_{out-CO_2} = 0.9997$	$R^2 = 0$
Hydrocarbon purity of captured natural gas	PSA	$y_{out-CH4} = -0.060\ln x_{in-CO_2} + 1.1594$	$R^2 = 0.9615$
	MS	$y_{out-CH4} = -0.072\ln x_{in-CO_2} + 1.1573$	$R^2 = 0.8890$
	LTF	$y_{out-CH4} = -0.025\ln x_{in-CO_2} + 1.0597$	$R^2 = 1$
	MDEA	$y = 0.9725$	$R^2 = 0$

3.4. Calculation Method of Unit Cost

The CO_2 capture and reinjection cost (CCRC) per unit volume of CO_2 gas can be calculated by the annual cost divided by the annual captured CO_2 gas. The annual cost includes two parts, namely the annual operating and maintenance cost, and the annual capital cost calculated by dividing the total capital cost equally over each year of the project [35]. The specific formulas are as follows. For comparison purposes, the unit CO_2 cost is expressed by the cost per 500 sm^3 CO_2 gas which is about one ton pure CO_2.

$$C_{lev} = C_{tca}/Q_{out-\mathrm{CO_2gas}}/365 \times 500 \tag{46}$$

$$C_{tca} = C_{annual} + O\&M_{annual} = \sum C_{unit} \times CRF + O\&M_{annual} \tag{47}$$

where C_{lev} is the CO_2 capture and reinjection cost per 500 Sm^3 CO_2 gas, US\$/500 Sm^3; C_{tca} is the total annual cost of CCRP, US\$; C_{annual} is the annual capital cost by dividing the total capital cost equally over each year of the project duration, US\$; CRF is the discount factor, which can be calculated according to project duration and the interest rate, in this study, it is assumed that the project lasts for 15 years, and the interest rate is 12%, hence the CRF of 0.1827 was applied.

4. Evaluation of the CCRPs in the CO_2 EOR and Storage Project in XinJiang Oilfield

4.1. Evaluation of the CCRPs Based on the Assumed Gas Production and CO_2 Purity

A sensitivity evaluation on the CCRP of the CO_2 EOR and storage project in XinJiang oilfield was conducted according to the possible gas production scale and CO_2 purity. It was assumed that the project lasts for 15 years, the discount rate is 12%, and the gas is produced at a scale of $(5-50) \times 10^4$ Sm^3/d with a CO_2 content varying in a range of 20–80 mol%. The unit cost, unit energy consumption, CCRE, and CO_2 capture purity of different CCRPs (as shown in Table 3) were calculated using the established evaluation model for CCRP, and the results are shown in Figure 6.

The calculated unit cost of CO_2 capture and unit cost of CO_2 capture and reinjection are shown in Figure 6a,b respectively, where the former covers the cost of equipment from the produced gas to the CO_2 capture system, while the latter further covers the cost of pressure boosting equipment for reinjection. It can be seen that both the unit capture cost and the unit capture and reinjection cost decrease with the increase of CO_2 content and gas production. The cost of capture accounts for the vast majority of the cost of the whole CCRP. By comparing these unit costs, the applicable CO_2 content of produced gas for different CCRPs can be obtained. The unit cost of the MDEA process is weakly sensitive to the CO_2 content in the produced gas, and it is economical at a low CO_2 content of 20–40 mol%. The unit cost of the SPA process is relatively low, and it has a large applicable CO_2 content range of $20-80$ mol%. The unit costs of MS and LTF processes are high, but decrease rapidly with CO_2 content increase. These two CO_2 capture processes are suitable for the conditions when the produced gas CO_2 contents are larger than 50 mol% and 80 mol% respectively.

Figure 6c,d show the unit energy consumptions of different CCRPs. It can be seen that the unit energy consumption is mainly decided by the CO_2 content in the produced gas. The higher the CO_2 content, the smaller the unit energy consumption. Similarly, the CO_2 capture process consumes most of the power of the whole CCRP. By comparison, the unit energy consumptions of SPA and MS processes are much lower than those of the other two. The unit energy consumption of the MDEA process is weakly affected by the CO_2 content in the produced gas, while the unit energy consumption of the LTF process is the most sensitive to the CO_2 content. When the CO_2 content of produced gas is larger than 40–60mol%, with the CO_2 liquefaction efficiency increase, the unit energy consumption of the LTF process will be lower than that of MDEA.

As shown in Figure 6e, the CCRE of the whole CCRP is also mainly affected by the CO_2 content in the produced gas. The higher the CO_2 content is, the higher the CCRE is. Among the four types of the CO_2 capture process, the CCRE of the PSA process is the highest. The CCRE of the MS process is lower than that of the PSA process, but it

increases quickly as the CO_2 content in the produced gas increases. At a low CO_2 content of 20–40 mol%, due to the low gas capture purity, a large part of CO_2 will be lost in the captured natural gas, resulting in a low CCRE of the MS process, even lower than that of the MDEA process. Relatively, the CCRE of the LTF process is low due to the high energy consumption and low CO_2 capture purity. At a low CO_2 content, the CCRE of the LTF process can be as low as 30%, while when the CO_2 content in the produced gas is larger than 60mol%, the CCRE of the LTF process can exceed that of the MDEA process. The CCRE of the MDEA process will be the lowest when the CO_2 content in the produced gas is above 60mol%.

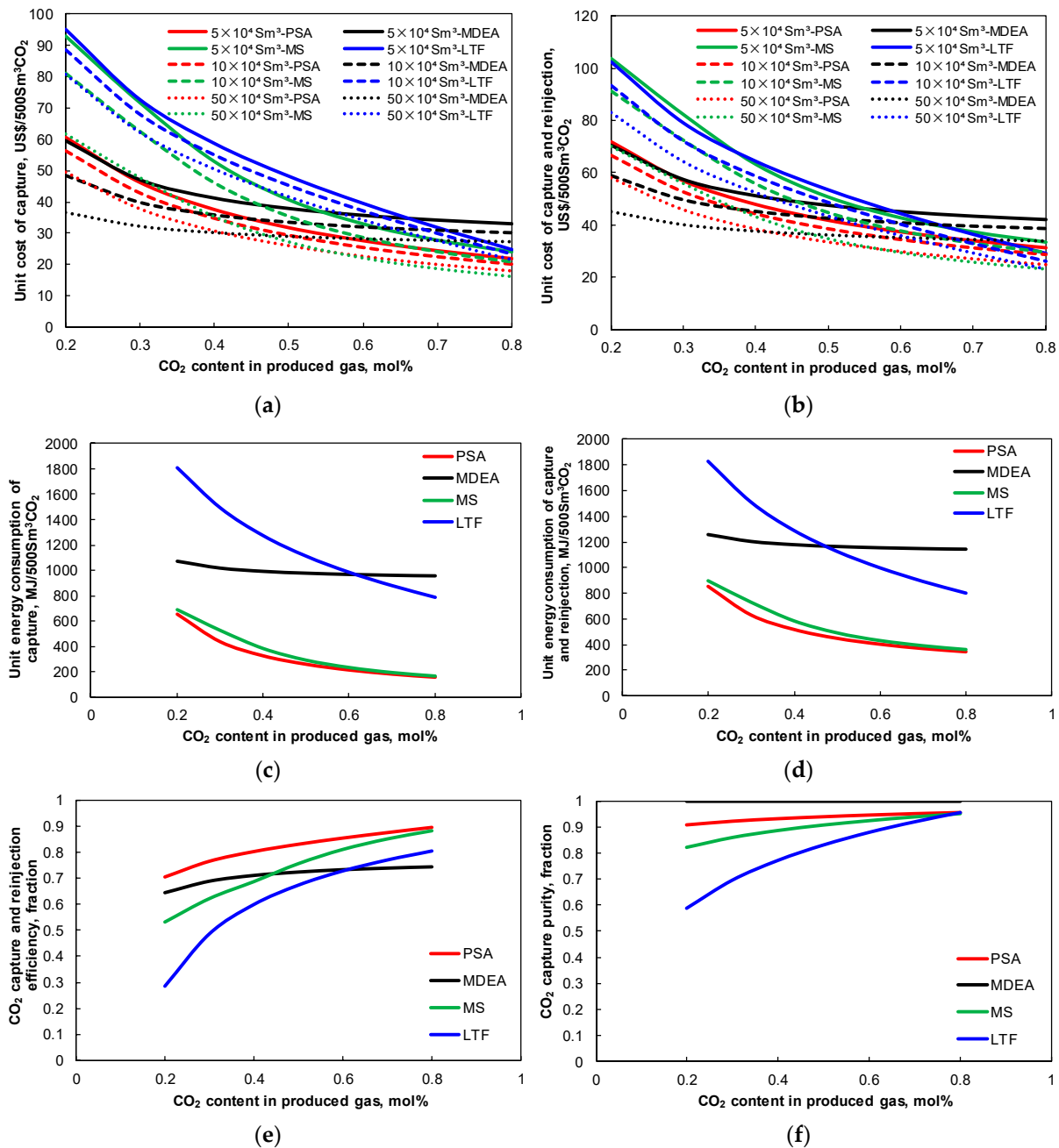**Figure 6.** Calculation results of the evaluation indicators of the CCRPs at different gas production conditions. (**a**) Unit cost of CO_2 capture; (**b**) Unit cost of CO_2 capture and reinjection; (**c**) Unit energy consumption of CO_2 capture; (**d**) Unit energy consumption of CO_2 capture and reinjection; (**e**) CO_2 capture and reinjection efficiency; (**f**) CO_2 capture purity.

Figure 6f shows the purity of CO_2 captured from the produced gas. The CO_2 purities captured by the MDEA and PSA processes all exceed 90 mol% when the CO_2 content in the produced gas is 20–80 mol%. However, for the MS and LTF processes, only when the CO_2 contents in the produced gas are more than 50 mol% and 70 mol%, respectively, the CO_2 capture purities can be larger than 90 mol%. The multi-stage membrane treatment can improve the CO_2 purity, while the heavy components liquefied with CO_2 are also conducive to miscible flooding.

When the produced gas is reinjected directly with necessary purchased pure CO_2, the unit cost, unit energy consumption, and CCRE of the DRM process are shown in Figure 7. Due to the simple process of DRM, both the unit cost and unit energy consumption are much lower than those of other CCRPs. The CCRE of the DRM process can be up to 70–93%, also larger than that of any other CCRPs. The DRM process demonstrates a strong attraction. Moreover, the unit cost of the DRM process increases with CO_2 content rise because compressing CO_2 needs more energy than natural gas.
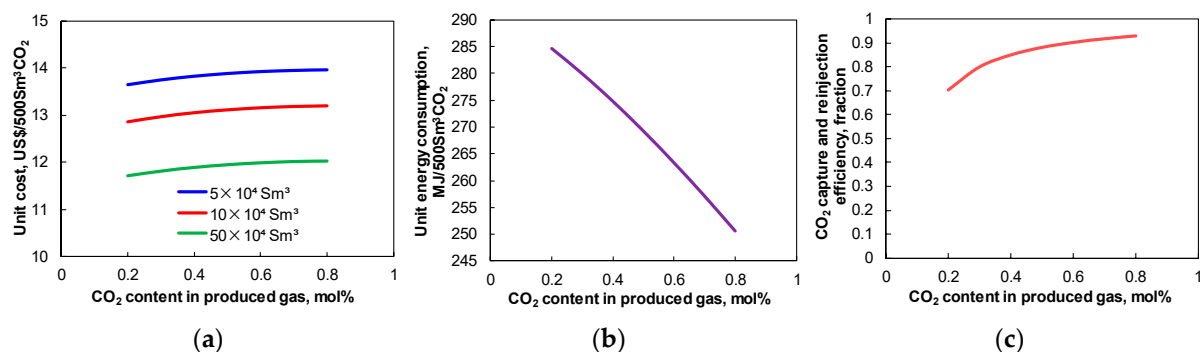

Figure 7. Calculation results of the evaluation indicators of the DRM process. (**a**) Unit cost; (**b**) Unit energy consumption; (**c**) CO_2 capture and reinjection efficiency.

4.2. Evaluation of the CCRPs Based on the Designed CO_2 Flooding Schemes

In order to optimize the CO_2 EOR and storage scheme in block 530, four times of CO_2 flooding were predicted by reservoir numerical simulation. In this part, five types of CCRPs are assessed and compared according to the predicted gas production.

4.2.1. CO_2 Injection Schemes and Predicted Gas Production

The CO_2 injection schemes and predicted gas productions in XinJiang oilfield are summarized in Table 4 and Figure 8. In the simulation of $CO_2 -$ EOR schemes, after CO_2 is injected into the ground, it interacts with formation water and crude oil, causing the composition and properties of liquid phase to be changed. Part of the injected CO_2 is dissolved in the oil underground and cannot be produced in gaseous form. CMG software was used to simulate the above process to obtain $CO_2 -$ EOR simulation cases. The four CO_2 flooding schemes are marked as cases A, B, C, and D, respectively. The CO_2 injection undergoes three stages: pressure build-up for 0.5 years, continuous gas injection for 4.5 years, and water-alternating-gas (WAG) injection for 10 years.

In four cases, the simulation results are various. (1) In case A, 139.93×10^4 t of CO_2 will be injected with a primary storage efficiency of 61.38%, and about 41.60×10^4 t of crude oil will be produced out with a CO_2–oil ratio of 3.36 tCO_2/t oil. The maximum gas production rate is expected to be 10×10^4 Sm^3/d, while the CO_2 content in the produced gas will be maintained at 65–76 mol% after the CO_2 breaks through in the production wells in the third year. (2) Case B has lower cumulative CO_2 injection and cumulative oil production, only 26.04×10^4 t and 26.93×10^4 t, respectively. CO_2 breakthrough of the production well occurs in the second year, and then the CO_2 content in the produced gas will gradually rise to more than 80mol %. (3) In case C, 108.22×10^4 t of CO_2 will be injected into 15 wells with a high storage efficiency of 79.85%, and 33.17×10^4 t of crude

oil will be produced out with a relatively higher CO_2–oil ratio of 3.26 tCO_2/t oil. CO_2 was produced in the first year, and the CO_2 content in produced gas can close to 90mol% after 5 years. (4) Case D has a similar CO_2 injection scale with case A, reaching 123.93×10^4 t, but has greater oil production of 49.49 t. CO_2 breaks through in the second year, and the CO_2 content can also be close to 90 mol %.

Table 4. Predicted results of four CO_2 flooding schemes for CO_2 EOR and storage project in XinJiang oilfield.

Scheme	Case A	Case B	Case C	Case D
Total CO_2 injection rate, 10^4 Sm^3/d	10–14	5–10	8–14	8–15
Total gas production rate, 10^4 Sm^3/d	0–10	0–3.7	0–4.5	0–7.8
CO_2 content in produced gas, %	65–76	56–88	20–90	40–90
Cumulative CO_2 injection, 10^4 t	139.93	80.83	108.22	123.93
Cumulative CO_2 production, 10^4 t	54.04	26.93	21.81	54.70
Primary CO_2 storage efficiency, %	61.38	66.68	79.85	55.86
Cumulative oil production, 10^4 t	41.60	26.04	33.17	49.49
Average CO_2-oil ratio, t CO_2/t oil	3.36	3.10	3.26	2.50
EOR, %	29.50	18.47	23.26	25.75
No of well group	9 injection wells	9 injection wells	15 injection wells	15 injection wells
Project period, year	15	15	15	15

Note: primary CO_2 storage efficiency refers to the ratio of the amount of stored CO_2 (=cumulative CO_2 injection—cumulative CO_2 production) and the cumulative CO_2 injection.
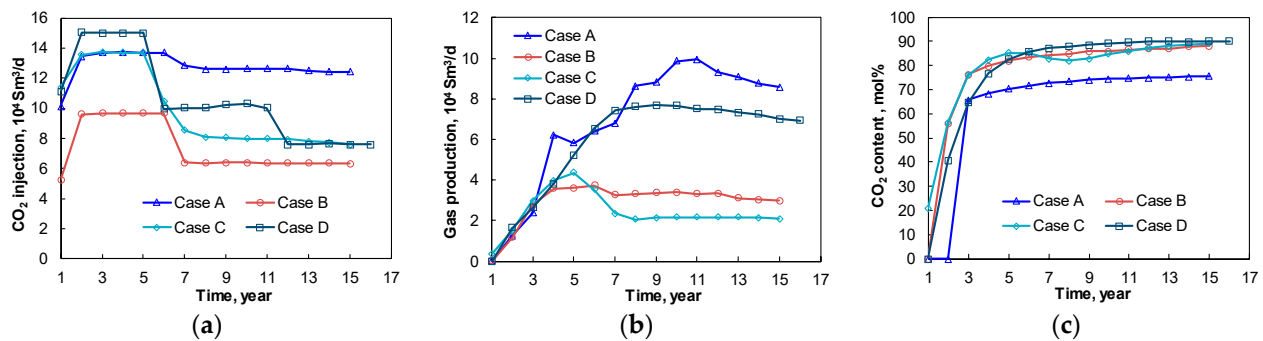

Figure 8. (**a**) Gas injection rate, (**b**) Gas production rate, and (**c**) CO_2 content in produced gas. The predicted gas injection and production in the CO_2 EOR and storage project in XinJiang oilfield.

Overall, case A has the largest CO_2 injection scale, while case D is the most attractive scheme because of the smallest CO_2–oil ratio and the little smaller gas production with the higher CO_2 content. For cases B and C, the CO_2 injection and gas production are small. Although their primary storage efficiencies are relatively high (66.68% and 79.85%, respectively), less amount of crude oil will be produced than that of cases A and D.

4.2.2. Comparison Analysis of the Different CCRPs

(1) Comparison between the different CCRPs

The best CO_2 injection scheme, case D, was taken as an example, and different CCRPs were compared and analyzed according to their technical and economic indicators calculated based on the predicted gas production of each year.

As shown in Figure 9a,b, as the CO_2 content in the produced gas increases with production, the unit CO_2 capture costs of different CCRPs decrease first and tend to be stable after a 5-year injection when the CO_2 content exceeds 80mol%. The unit CO_2 capture costs of PSA,

MS, and LTF processes become close, varying in a range of 17.63–20.35 US$/500 Sm^{3}CO$_2$, while the unit CO$_2$ capture cost of the MDEA process maintains at a high level of 28.46–31.17 US$/500 Sm^{3}CO$_2$. When the cost of the injection process is further involved, the unit costs of CCRPs will increase by about 10 US$/500 Sm^3 CO$_2$, except for the unit cost of the LTF process, which is only improved by 3–4 US$/500 Sm^{3}CO$_2$ due to the low injection cost of liquid CO$_2$. However, the cheapest way to dispose of the produced gas is to reinject the produced gas directly. The unit cost of the DRM process is only 13.58–15.64 US$/500 Sm^3 CO$_2$.
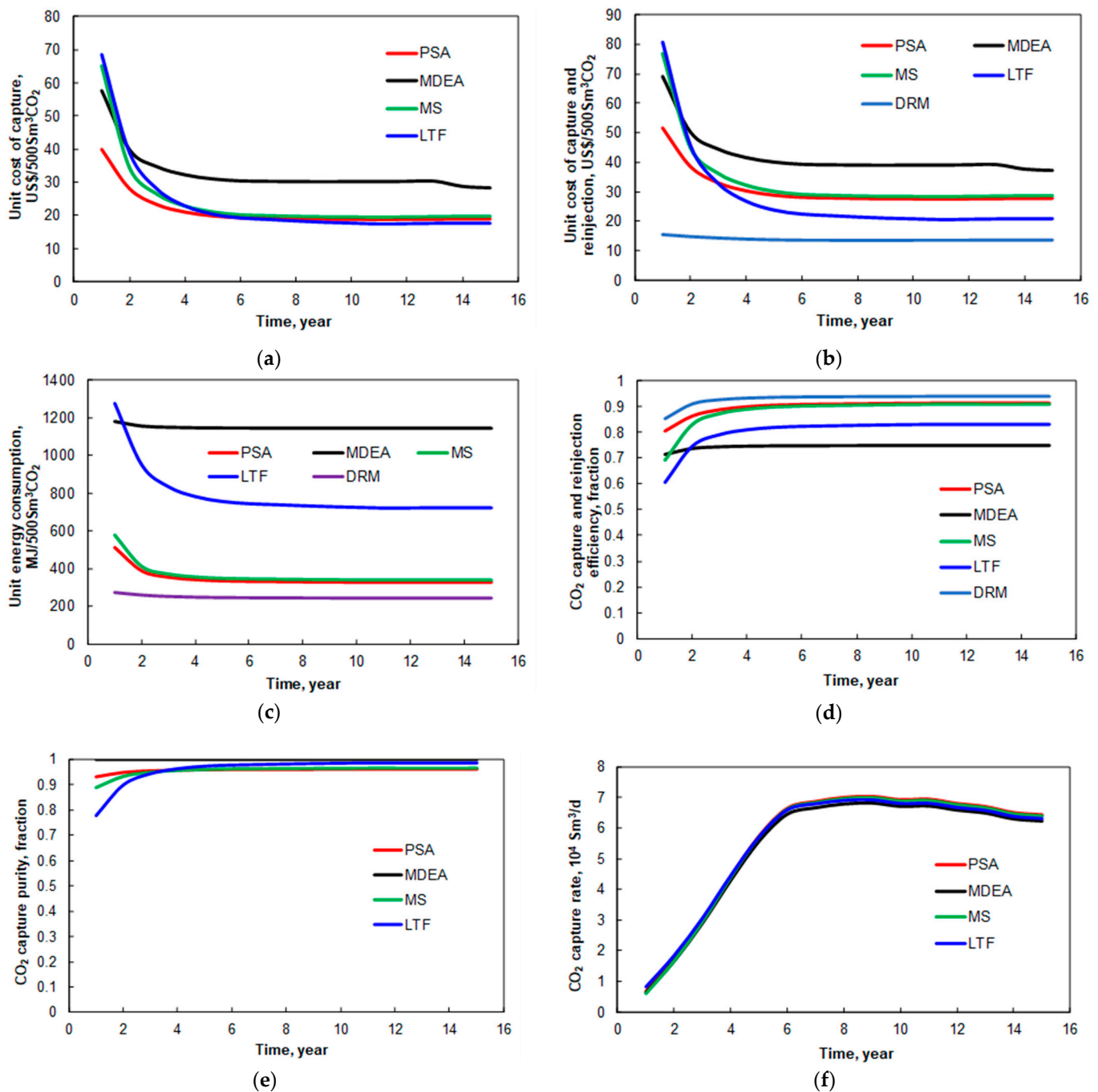
Figure 9. The calculated evaluation indicators of different CCRPs based on the predicted production of case D. (**a**) Unit cost of CO$_2$ capture; (**b**) Unit cost of CO$_2$ capture and reinjection; (**c**) Unit energy consumption; (**d**) CO$_2$ capture and reinjection efficiency (CCRE); (**e**) CO$_2$ capture purity; (**f**) CO$_2$ capture rate.

Figure 9c shows the unit energy consumptions of different CCRPs with time. The unit energy consumptions of PSA, MS, and LTF processes decrease quickly in the first 2–3 years and tend to be stable, while the unit energy consumptions of MDEA and DBM processes always remain stable. The order of unit energy consumptions of different CCRPs is MDEA > LTF > MS ≈ PSA > DRM (1143, 721, 342, 328, and 244 MJ/500 Sm^3, respectively, after 15 years of injection). A high energy consumption usually means a large amount of additional CO_2 emissions and a low effective CO_2 capture efficiency; hence, the ranking of CCREs of different CCRPs is DRM > MS ≈ PSA > LTF > MDEA (93.97%, 91.48%, 90.96%, 83.10%, and 74.86%, respectively, 15 years later), as shown in Figure 9d.

For the CO_2 capture purity, as shown in Figure 9e, only in the MDEA and PSA processes can it reach 90 mol% in the first 2 years, while the CO_2 capture purity of the LTF process is as low as 77.69% at the beginning. After 4 years of production, the CO_2 capture purities of different CCRPs become stable with an order of MDEA > LTF > PSA ≈ MS > 90 mol%. For the CO_2 capture rate, only a little difference is between different CCRPs because of the high CO_2 content in the produced gas, as shown in Figure 9f.

Based on the above analysis, it can be seen that the DRM process is the best way to deal with the produced gas. However, before reinjection, the produced gas should be mixed with the purchased pure CO_2 if necessary to meet CO_2 purity and injection amount requirements. As shown in Figure 10a, when the produced gas is mixed with the purchased pure CO_2 to meet the required CO_2 purity of 90 mol%, no more than 8×10^4 Sm^3/d of pure CO_2 is needed, and with the increase of gas production and decrease of required injection amount, no additional pure CO_2 will be needed 10 years later. However, when the produced gas is mixed with pure CO_2 according to the required CO_2 purity, the total amount of produced gas and pure CO_2 is still less than the designed amount. Hence, more purchased pure CO_2 is needed, which will make the CO_2 content in the mixed gas up to 91–95 mol%, as shown in Figure 10b.
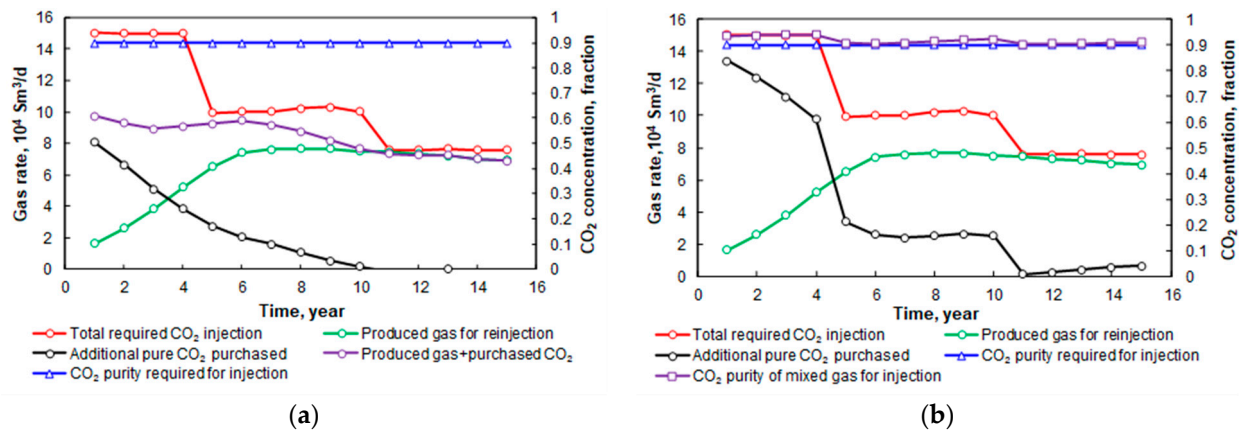

(**a**)　　　　　　　　　　　　　　　(**b**)

Figure 10. (**a**) Based on the required CO_2 purity. (**b**) Based on the required injection amount. Two types of produced gas mixed with the purchased pure CO_2 in the DRM process of case D.

(2) Comparison of CCRPs between the different cases

Besides case D, the other three cases of CO_2 flooding were also assessed to study the influence of gas production characteristics on selecting the optimal CCRP. The evaluation indicators of all CCRPs of all cases are summarized in Table 5.

For case A, the order of different CCRPs is MDEA > MS ≈ PSA ≈ LTF > DRM according to the unit costs of CCRPs when the CO_2 content in the produced gas has reached stable after several years of production. Due to the stable CO_2 content of 65–76 mol% in the produced gas, the CO_2 capture purity, unit energy consumption, and CCRE are all kept stable during the project. However, it is not easy to design the DRM process. On the one side, the amount of mixed gas will be much larger than the required amount if the produced gas is mixed with the purchased pure CO_2 based on the required CO_2

purity. On the other side, the CO_2 purity of mixed gas will be lower than 90 mol% during most of the project time if the produced gas is mixed with the purchased pure CO_2 based on the required injection amount. For this case, the MS, PSA, or LTF process may be an assistant selection.

For case B, the unit costs of different CCRPs are in the order of MDEA > MS > PSA > LTF > DRM. The CO_2 content in the produced gas is 56–88 mol%, and after three years of production, the CO_2 content can maintain above 80 mol%. At such a high CO_2 content, the unit CO_2 capture cost of the LTF process is close to that of MS and PSA processes, while the total unit cost of the LTF process is lower than that of any other capture processes because of the low injection cost of liquid CO_2. Besides, the LTF process has the second-high CO_2 capture purity, although the unit energy consumption is high and the CCRE is as low as about 80%. This case is similar to case D. The DRM process is the most attractive option, and when the produced gas is mixed with pure CO_2 according to the required injection amount, the CO_2 content of the mixed gas can be high up to 92–95 mol%.

For case C, the unit costs of different CCRPs have the same order as that of case B. In this case, the injected CO_2 will breakthrough in the first year, and the CO_2 content in the produced gas is only 20 mol%; only in the fourth year will the CO_2 content exceed 80 mol%. Hence, in the early stage of the project, the unit cost of CO_2 capture will be very high. For the DRM process, a large amount of pure CO_2 should be purchased to mix with the produced gas, which will lead to a high CO_2 purity of mixed gas in a range of 95–98 mol%.

Table 5. Summary of evaluation indicators of all CCRPs of all cases.

CO_2 Flooding Scheme	Type of CCRP	Unit Cost of Capture, US$/500 Sm³$CO_2$	Unit Cost of Capture and Reinjection, US$/500 Sm³$CO_2$	Unit Energy Consumption, MJ/500 Sm³CO_2	CO_2 Capture and Reinjection Efficiency, %	CO_2 Capture Purity, %
Case A	SPA	21–25	30–36	358–386	87–89	95
	MDEA	31–41	39–51	1148–1154	74	99.97
	MS	23–35	31–45	375–409	84–87	93–95
	LTF	26–39	29–46	843–939	75–79	90–94
	DRM	7–9 *	13–15	253–260	91–93	80–94 **
Case B	SPA	21–34	31–46	332–422	84–91	94–96
	MDEA	33–55	43–67	1143–1161	73–75	99.97
	MS	24–48	34–60	345–454	79–91	92–96
	LTF	21–55	26–68	735–1049	71–83	86–98
	DRM	9–10 *	15–16	245–266	90–94	92–95 **
Case C	SPA	20–95	31–109	330–830	71–91	91–96
	MDEA	35–238	45–94	1142–1254	65–75	99.97
	MS	23–166	36–180	344–884	63–91	83–96
	LTF	21–182	28–243	727–1803	31–83	60–98
	DRM	8–14 *	15–20	244–284	70–94	95–97 **
Case D	SPA	19–40	28–51	328–513	80–91	93–96
	MDEA	28–58	37–69	1142–1180	71–75	99.97
	MS	19–65	28–77	341–575	69–91	89–96
	LTF	18–69	21–81	719–1276	61–83	78–99
	DRM	8–10 *	14–16	244–274	85–94	91–95 **

Note: the data marked by * are the pretreatment costs of the produced gas in the DRM process; the data marked by ** are the CO_2 contents of the produced gas after being mixed with the purchased pure CO_2 in the DRM process.

By comparing the four cases of CO_2 flooding, it can be seen that (1) the DRM process is the best selection, but if the gas production is large and has a low-medium CO_2 content, the DRM process may bring new issues such as more blocks are needed for gas injection or the

CO_2 content of the mixed gas cannot meet the required CO_2 purity. (2) The MDEA process can be excluded because of its high cost and energy consumption during most project times. (3) When the CO_2 content in the produced gas is above 80 mol%, the LTF process is an attractive option, while when the CO_2 content is lower than 80 mol%, the PSA process is better than the MS process. Because of the considering of the probable adjustment of CO_2 injection during the project, a more flexible and applicable CCRP is recommended as the following: the DRM process is selected as the main CCRP, and the PSA process is chosen as an assistant option that has a wide range of applicable CO_2 content in the produced gas.

5. Conclusions

(1) For the CO_2 EOR and storage project in XinJiang oilfield, a technical and economic evaluation model of CCRP was established based on the basic equipment units involved in the process, which can be applicable for any flexibly designed CCRPs. The evaluation indicators such as unit cost, unit energy consumption, CO_2 capture efficiency, and CO_2 capture purity of each equipment unit and the whole process can be calculated and used as the basis for the optimization of CCRP.

(2) The results of sensitivity evaluation of CCRPs show that with the increase of gas production rate and CO_2 content in the produced gas, the unit cost and energy consumption of CCRP will decrease, while the CCRE and CO_2 capture purity will increase. The MDEA and LTF processes have large unit energy consumptions, while the PSA process has a large CCRE and a high CO_2 capture purity. In terms of the unit cost, the applicable CO_2 contents in the produced gas for the MDEA, PSA, MS, and LTF processes are <20–40 mol%, >20–80 mol%, >50 mol%, and >80 mol% respectively, which are consistent with published studies. The DRM process is the most attractive selection because of its simple process, low unit cost, and high CCRE.

(3) According to the designed CO_2 flooding schemes in XinJiang oilfield, different CCRPs were assessed. Different CCRPs have different advantages at different stages of the project. For the case of high gas injection and high gas production with a relatively low CO_2 content, the DRM process is hard to apply. All or part of the produced gas may need to be purified by PSA, MS, or LTF processes, of which the PSA process has the widest applicable CO_2 content range. For the case of high gas injection and low gas production with high CO_2 content, the DRM process can be applied by mixing the produced gas with pure CO_2 according to the required injection amount. Considering the probable adjustment of the CO_2 injection scheme, a flexible and applicable CCRP is recommended to select the DRM process as the main CCRP associated with the PSA process as an assistant option.

(4) In general, the implementation of CCS in the oil field is economically rewarding, and CO_2 can be stored permanently and safely. Besides, a large number of CO_2 flooding projects around the world have also proved that this is the most feasible commercialization model. Therefore, a reasonable CCRP after enough evaluation can provide a guarantee for the CO_2 EOR and storage project of XinJiang Oilfield. Furthermore, the success of the XinJiang oilfield provides a reference for the process optimization and environmental protection indicators of the CCS technology in China.

Institutional Review Board Statement: Not applicable.

Informed Consent Statement: Not applicable.

Data Availability Statement: The data presented in this study are available.

Conflicts of Interest: The authors declare no conflict of interest.

Abbreviations and Nomenclature

Abbreviations

CA	Chemical absorption
CCRE	CO_2 capture and reinjection efficiency
CCRP	CO_2 capture and reinjection process
CCS	CO_2 capture and storage
CCUS	CO_2 capture, utilization, and storage
CFGR	combustion and flue gas reinjection
DRM	direct reinjection mixed
EOR	enhanced oil recovery
LTF	low-temperature fractionation
MDEA	methyldiethanolamine
MS	membrane separation
PSA	pressure swing adsorption

Nomenclature

C_{sep}	capital cost of gas–liquid separator (US\$)
M_{train}	mass flow rate of disposal gas (t/d)
C_{mol}	capital cost of molecular sieve (US\$)
C_{comp}	total capital cost of compressor (US\$)
m_{train}	mass flow rate of CO_2 gas in each compressor unit (kg/s)
N_{train}	number of parallel compressors (dimensionless)
m_{CO_2}	CO_2 mass flow rate (t/d)
$P_{in-comp}$	inlet pressure of compressor (MPa)
$P_{out-comp}$	outlet pressure of compressor (MPa)
W_{comp}	compressor power (kW)
Z_s	average compression factor of CO_2 at each stage (dimensionless)
$T_{in-comp}$	inlet temperature of compressor (K)
M_{CO_2gas}	molar mass of CO_2 gas (kg/kmol)
η_{comp}	efficiency of compressor (dimensionless)
k_s	average heat capacity ratio of CO_2 at each stage of compressor (dimensionless)
CR	optimal compression ratio (dimensionless)
N_{stage}	number of compression stages (dimensionless)
C_{pump}	capital cost of booster pump (US\$)
W_{pump}	booster pump power (kW)
$P_{out-pump}$	outlet pressure of booster pump (MPa)
$P_{in-pump}$	inlet pressure of booster pump (MPa)
ρ_{l-CO_2}	density of liquid CO_2 (kg/m^3)
η_{pump}	efficiency of booster pump (dimensionless)
W_{PSA-ad}	mass of adsorbent in PSA module (kg)
Q_{PSA-g}	flow rate of the feed gas in the adsorption tower of PSA module (m^3/s)
t_{PSA-ad}	adsorption time of single bed operation of tower in PSA module (s)
y_{PSA-CO_2}	CO_2 mole fraction of the feed gas in PSA module (dimensionless)
Δq_{PSA}	adsorption capacity in PSA module (kg/kg)
$n_{PSA-bed}$	number of beds for continuous adsorption in a single tower in PSA module (dimensionless)
H_{PSA}	height of the tower in PSA module (m)
v_{PSA-g}	gas flow speed in adsorption tower of PSA module (m/s)

ρ_{PSA-ad}	adsorbent density in PSA module (kg/m^3)
D_{PSA}	diameter of the tower in PSA module (m)
$n_{PSA-tower}$	number of towers in PSA module (dimensionless)
$C_{PSA-tower}$	capital cost of towers in PSA module (US$)
C_{PSA-pc}	unit height capital cost of the tower in PSA module (US$/m)
C_{PSA-ad}	purchase cost of adsorbent in PSA module (US$)
P_{PSA-ad}	unit cost of adsorbent in PSA module (US$/kg)
C_{PSA}	capital cost of the PSA module (US$)
W_{PSA}	power of the PSA module (kW)
A_m	film area in MS module (m^2)
Y_{MS-F}	mole fraction of high-speed group (CO_2) in feed gas in MS module (dimensionless)
Y_{MS-R}	mole fraction of the high-speed group in the nonpenetrating gas in MS module (dimensionless)
Y_{MS-1}	mole fraction of the high-speed group in the permeation gas in MS module (dimensionless)
Q_{MS-P}	flow rate of permeation gas in MS module (kmol/s)
R_{MS-f}	weighted average permeation velocity of the high-speed group in MS module (m/s)
P_{MS-1}	total pressure on the low-pressure side of the membrane in MS module (bar)
P_{MS-2}	total pressure on the high-pressure side of the membrane in MS module (bar)
C_M	capital cost of MS device (US$)
I_m	cost of membrane material in MS device (US$)
I_{mf}	cost of membrane frame in MS device (US$)
K_m	membrane material cost of unit film area (US$/m^2)
K_{mf}	membrane frame cost of unit film area (US$/m^2)
C_{MS}	capital cost of MS module (US$)
W_{MS}	power of MS module (kW)
C_{hx}	capital cost of heat exchanger (US$)
A_{hx-p}	actual heat exchange area in heat exchanger (m^2)
Q_{hx}	heat flow in heat exchanger (kJ/h)
m_{hf}	mass flow rate of hot fluid in heat exchanger (kg/h)
C_p	specific heat capacity of fluid in heat exchanger in heat exchanger (kJ·kg^{-1}·°C^{-1})
Δt_{hx}	temperature change of hot fluid in heat exchanger (°C)
K_{hc}	heat transfer coefficient between the hot fluid and the cold fluid in heat exchanger (W·m^{-2}·°C^{-1})
ΔT_m	logarithmic mean temperature changes of heat exchanger (°C)
T_{HI}	hot fluid temperature at the inlet of the heat exchanger (°C)
T_{HO}	hot fluid temperature at the outlet of the heat exchanger (°C)
T_{CI}	cold fluid temperature at the inlet of the heat exchanger (°C)
T_{CO}	cold fluid temperature at the outlet of the heat exchanger (°C)
W_{hx}	power of heat exchanger (kW)
C_{LTF}	capital cost of LTF module (US$)
W_{LTF}	power of LTF module (kW)
D_{CA-ab}	diameter of absorption tower in CA module (m)
V_{CA-ab}	flow rate of feed gas in the absorption tower in CA module (m^3/h)
v_{CA-ab}	gas flow velocity in the adsorption tower in CA module (m/s)
H_{CA-ab}	cumulative height of absorption towers in CA module (m)
m_{CA-CO_2}	mass flow rate of CO_2 gas in CA module (kg/h)
K_{Ga}	mass transfer coefficient in CA module (kmol·m^{-3}·h^{-1}·atm^{-1})
Y_{CO_2-inab}	CO_2 content of inlet gas in absorption tower (g/m^3)
$Y_{CO_2-outab}$	CO_2 content of outlet gas in absorption tower (g/m^3)
A_{CA-t}	cross–section area of absorption tower in CA module (m^2)
ΔP_{CA-m}	driving pressure difference in the absorption tower of CA module (atm)
C_{CA-ab}	cost of unit height tower in CA module (US$/m)
C_{CA-abt}	capital cost of absorption tower in CA module (US$)
D_{CA-de}	diameter of the desorption tower in CA module (m)
V_{CA-de}	flow rate of feed gas in the desorption tower in CA module (m^3/h)
v_{CA-de}	gas flow velocity in the desorption tower in CA module (m/s)

N_{CA-t}	total number of theoretical plates in desorption tower in CA module (dimensionless)
C_{CA-de}	tower cost of a single plate of desorption towers in CA module (US$)
C_{CA-det}	capital cost of desorption tower in CA module (US$)
M_{MDEA}	required circulation amount of MDEA solution (t)
C_s	purchase cost of MEDA solution (US$)
C_{us}	unit cost of MEDA solution (US$/t)
C_{CA}	capital cost of CA module (US$)
W_{CA}	power of CA module (kW)
$O\&M_{annual}$	annual running cost of CCRP (US$)
C_{unit}	capital cost of equipment unit (US$)
M_{factor}	ratio of annual maintenance cost to total infrastructure cost (dimensionless)
W_{unit}	power of equipment unit (kW)
F_{elec}	electricity price (US$/kWh)
Q_{in-gas}	gas flow rate at the inlet of equipment unit (Sm^3/d)
x_{in-CO_2}	CO_2 content at the inlet of equipment unit (dimensionless)
Q_{in-CO_2}	pure CO_2 gas flow rate at the inlet of equipment unit (Sm^3/d)
$Q_{out-gas}$	gas flow rate at the outlet of equipment unit (Sm^3/d)
Q_{out-CO_2gas}	CO_2 gas flow rate at the outlet of equipment unit (Sm^3/d)
$Q_{out-CH4gas}$	CH_4 gas flow rate at the outlet of equipment unit (Sm^3/d)
x_{out-CO_2}	CO_2 purity of CO_2 gas flow at the outlet of equipment unit (dimensionless)
$y_{out-CH4}$	CH_4 purity of CH_4 gas flow at the outlet of equipment unit (dimensionless)
Q_{out-CO_2}	pure CO_2 gas flow rate at the outlet of equipment unit (Sm^3/d)
$Q_{power-CO_2}$	energy consumption equivalent CO_2 emission of equipment unit (Sm^3/d)
η	CO_2 capture efficiency of the capture module (dimensionless)
M_{coal}	coal consumption required for unit power generation (kg/kWh)
E_{CO_2}	CO_2 emissions per unit coal by burning (kg CO_2/kg coal)
t_u	unit time (h)
ρ_{CO_2}	density of CO_2 gas (kg/m^3)
C_{lev}	CO_2 capture and reinjection cost per 500 Sm^3 CO_2 gas (US$/500$Sm^3$)
C_{tca}	total annual cost of CCRP (US$)
C_{annual}	annual capital cost by dividing the total capital cost equally over each year of the project duration (US$)
CRF	the discount factor (dimensionless)

References

1. Ren, S.R.; Li, D.Y.; Zhang, L.; Huang, H. Leakage Pathways and Risk Analysis of Carbon Dioxide in Geological Storage. *Acta Pet. Sin.* **2014**, *35*, 591–601. (In Chinese with English abstract)
2. Qin, J.X.; Han, H.S.; Liu, X.L. Application and enlightenment of carbon dioxide flooding in the United States of America. *Pet. Explor. Dev.* **2015**, *42*, 209–216. [CrossRef]
3. Sourisseau, K.; Ibrahim, I.; Al-Jabri, A.; Wetzels, G. Surface facilities considerations for the production of a large sour gas resource and the injection of sour and/or acid gas. In Proceedings of the Abu Dhabi International Petroleum Exhibition and Conference, Abu Dhabi, United Arab Emirates, 13–15 October 2000.
4. Zainal, Z.A.; Mahadzir, M.M. Experimental study of hydrodynamic characteristics and CO_2 absorption in producer gas using CaO-sand mixture in a bubbling fluidized bed reactor. *Int. J. Chem. React. Eng.* **2011**, *9*, 154–156.
5. Adewole, J.K.; Ahmad, A.L. Process modeling and optimization studies of high pressure membrane separation of CO_2 from natural gas. *Korean J. Chem. Eng.* **2016**, *33*, 2998–3010. [CrossRef]
6. Liu, B.L. *Experimental Study of Low-Temperature and Pressure Swing Adsorption Removal Carbon Dioxide Gas from Natural Gas*; Dalian University of Technology: Dalian, China, 2015. (In Chinese with English abstract)
7. Torp, T.A.; Brown, K.R. CO_2 underground storage costs as experienced at Sleipner and Weyburn. In Proceedings of the 7th International Conference on Greenhouse Gas Control Technologies, Vancouver, BC, Canada, 5 September 2004.
8. Ma, P.F.; Han, B.; Zhang, L.; Xiong, X.Q.; Shen, X.X.; Zhang, X.; Ren, S.R. Disposal scheme of produced gas and CO_2 capture for re-injection in CO_2 EOR. *Chem. Ind. Eng. Prog.* **2017**, *36*, 533–539. (In Chinese with English abstract)
9. Sun, R.Y.; Ma, X.H.; Wang, S.G. CO_2 injection technology in Jilin Oilfield. *Pet. Plan. Eng.* **2013**, *24*, 1–6. (In Chinese with English abstract).
10. Zhang, L.; Li, X.; Ren, B.; Cui, G.D.; Zhang, Y.; Ren, S.R.; Chen, G.L.; Zhang, H. CO_2 storage potential and trapping mechanisms in the H-59 block of Jilin oilfield China. *Int. J. Greenh. Gas Control* **2016**, *49*, 267–280. [CrossRef]
11. Zhang, L.; Ren, B.; Huang, H.D.; Li, Y.Z.; Ren, S.R.; Chen, G.L.; Zhang, H. CO_2 EOR and storage in Jilin Oilfield China: Monitoring program and preliminary Results. *J. Pet. Sci. Eng.* **2015**, *125*, 1–12. [CrossRef]

12. Zhang, L.; Yang, C.H.; Niu, B.L.; Ren, S.R. *EOR Principles and Application of CO₂ Flooding*; Press of China University of Petroleum: Qingdao, China, 2017. (In Chinese)

13. Yu, B.Y.; Zhao, G.P.; An, R.D.; Chen, J.M.; Tan, J.X.; Li, X.Y. Study on China's carbon emission path under the carbon neutral target. *J. Beijing Inst. Technol. (Soc. Sci. Ed.)* **2021**, *23*, 17–24. (In Chinese with English abstract)

14. Kwak, D.H.; Yun, D.; Binns, M.; Yeo, Y.K.; Kin, J.K. Conceptual process design of CO₂ recovery plants for enhanced oil recovery applications. *Ind. Eng. Chem. Res.* **2014**, *53*, 14385–14396. [CrossRef]

15. Zhou, D.B. *EOR Natural Gas CO₂ Separation Process Simulation Study*; Qingdao University of Science and Technology: Qingdao, China, 2014. (In Chinese with English abstract)

16. Ciferno, J.P.; DiPietro, P.; Tarka, T. *An Economic Scoping Study for CO₂ Capture Using Aqueous Ammonia*; Final Report; National Energy Technology Laboratory, US Department of Energy: Pittsburgh, PA, USA, 2005.

17. Kleme, J.; Bulatov, I.; Cockerill, T. Techno-economic modeling and cost functions of CO₂ capture processes. *Comput. Chem. Eng.* **2007**, *31*, 445–455. [CrossRef]

18. Tuinier, M.J.; Hammers, H.P.; van Sint Annaland, M. Techno-economic evaluation of cryogenic CO₂ capture—A comparison with absorption and membrane technology. *Int. J. Greenh. Gas Control* **2011**, *5*, 1559–1565. [CrossRef]

19. Huang, Y.P.; Rebennack, S.; Zheng, Q.P. Techno-economic analysis and optimization models for carbon capture and storage: A survey. *Energy Syst.* **2013**, *4*, 315–353. [CrossRef]

20. Zhang, Z.H. Techno-economic assessment of carbon capture and storage facilities coupled to coal-fired power plants. *Energy Environ.* **2015**, *26*, 1069–1080. [CrossRef]

21. Zohrabian, A.; Majoumerd, M.M.; Soltanieh, M.; Sourena, S. Techno-economic evaluation of an integrated hydrogen and power co-generation system with CO₂ capture. *Int. J. Greenh. Gas Control* **2016**, *44*, 94–103. [CrossRef]

22. Zhai, M.Y.; Lin, Q.G.; Zhong, L.F.; Pi, J.W.; Wang, W.S. Economic assessment of carbon capture and storage combined with utilization of deep saline water. *Mod. Chem. Ind.* **2016**, *36*, 8–12. (In Chinese with English abstract)

23. Hu, B.; Zhai, H. The cost of carbon capture and storage for coal-fired power plants in China. *Int. J. Greenh. Gas Control* **2017**, *65*, 23–31. [CrossRef]

24. Liu, J.J.; Zhao, D.Y.; Tian, Q.H.; Li, Z.M. Modeling and optimization of the whole process of CO₂ capture, transportation, oil displacement and storage. *Oil Gas Field Surf. Eng.* **2018**, *37*, 1–5. (In Chinese with English abstract)

25. Decardi-Nelson, B.; Liu, S.; Liu, J.F. Improving flexibility and energy efficiency of post-combustion CO₂ capture plants using economic model predictive control. *Processes* **2018**, *6*, 135. [CrossRef]

26. Yun, S.; Oh, S.Y.; Kim, J.K. Techno-economic assessment of absorption-based CO₂ capture process based on novel solvent for coal-fired power plant. *Appl. Energy* **2020**, *268*, 114933. [CrossRef]

27. Gui, X.; Wang, C.W.; Yun, Z.; Zhang, L.; Tang, Z.G. Research progress of pre-combustion CO₂ capture. *Chem. Ind. Eng. Prog.* **2014**, *33*, 1895–1901. (In Chinese with English abstract)

28. Li, Q.F.; Lu, S.J.; Liu, X.D.; Zhang, J. Experimental research of absorbing carbon dioxide from flue gas by MEA-MDEA mixed amine solutions. *Appl. Chem. Ind.* **2010**, *39*, 1127–1131. (In Chinese with English abstract)

29. Ahmad, A.L.; Adewole, J.K.; Leo, C.P.; Ismail, S.; Sultan, A.S.; Olatunji, S.O. Prediction of plasticization pressure of polymeric membranes for CO₂ removal from natural gas. *J. Membr. Sci.* **2015**, *480*, 39–46. [CrossRef]

30. Algharaib, M.; Al-Soof, N. Economical modeling of CO₂ capturing and storage projects. SPE 120815-MS. In Proceedings of the SPE Saudi Arabia Section Technical Symposium, Al-Khobar, Saudi Arabia, 10–12 May 2008.

31. Peters, M.S.; Timmerhaus, K.D.; West, R.E. *Plant Design and Economics for Chemical Engineers*; McGraw-Hill: New York, NY, USA, 1968.

32. Dong, X.; Han, P.; Yang, Z.; Xie, S.; Zhen, K. *Pilot Field Test of Carbon Dioxide Flooding in Daqing Oilfield*; Petroleum Industry Press: Beijing, China, 1999. (In Chinese)

33. Zhang, Y. *Research on CO₂-EOR and Geological Storage in Caoshe Oilfield, Jiangsu*; China University of Petroluem: Qingdao, China, 2010. (In Chinese with English abstract)

34. Hendriks, C.; Graus, W.; van Bergen, F. *Global Carbon Dioxide Storage Potential and Costs*; Ecofys: Utrecht, The Netherlands, 2004.

35. McCollum, D.L. *Techno-Economic Models for Carbon Dioxide Compression, Transport, and Storage*; University of California: Davis, CA, USA, 2006.

36. GHG IEA. *Transmission of CO₂ and Energy*; IEA Greenhouse Gas R&D Programme, Report PH4/6; IEA: Paris, France, 2002.

37. Han, Y.J.; Wang, S.L.; Zhang, P.Y.; Piao, P.Y. Status and progress of CO₂ separation and capture technology. *Nat. Gas Ind.* **2009**, *29*, 79–82. (In Chinese with English abstract)

38. Chen, D.Y. *Remove Carbon Dioxide by PSA*; Nanjing Tech University: Nanjing, China, 2003. (In Chinese with English abstract)

39. Yang, H.Y. *Research on Adsorbents for Separation of the CH₄/CO₂ Mixture*; Northeast Agricultural University: Harbin, China, 2013. (In Chinese with English abstract)

40. Meng, D. Structure Design and Stress Analysis of PSA Absorption Tower. *Petro-Chem. Equip.* **2010**, *39*, 33–36. (In Chinese with English abstract)

41. Zhou, F. Design of CO₂ absorption tower. *Guangdong Chem. Ind.* **2014**, *41*, 245–246. (In Chinese with English abstract)

42. Zhao, L.; Menzer, R.; Riensche, E.; Blum, L.; Stolten, D. Concepts and investment cost analyses of multi-stage membrane systems used in post-combustion processes. *Energy Procedia* **2009**, *1*, 269–278. [CrossRef]

43. Su, Y.; Hu, L.; Liu, M.S. Gas membrane separation technology and application. *Chem. Eng. Oil Gas* **2001**, *30*, 113–116. (In Chinese with English abstract)

44. Shi, M.Z.; Wang, Z.Z. *Principle and Design of Heat Exchangers*; Southeast University Press: Nanjing, China, 2009. (In Chinese)
45. Peng, Y.X. Coupling of distillation and low temperature stripping—A new output gas recovery technology in CO_2 flooding process in oilfields. *Reserv. Eval. Dev.* **2012**, *2*, 42–47. (In Chinese with English abstract)
46. Zhang, X.F. Calculation of effective height of chemical absorption packed tower. *Chem. Eng. Des. Commun.* **1995**, *21*, 42–46. (In Chinese with English abstract)
47. Liao, H.; Zhao, G.X.; Ma, B.Q. Design of HCl absorber for a 100 kt/a Deacon process. *Chem. World* **2015**, *56*, 653–657. (In Chinese with English abstract)
48. Chen, J.; He, G.; Liu, J.; Liu, J. Measurement for the absorption rate of CO_2 by aqueous MDEA solution. *J. Tsinghua Univ. (Sci. Technol.)* **2001**, *41*, 28–30. (In Chinese with English abstract)
49. Liu, Y.Z.; Shen, H.Y. *Carbon Dioxide Emission Reduction Process and Technology–Solvent Absorption Method*; Chemical Industry Press: Beijing, China, 2013. (In Chinese)
50. Li, T. *Study on Energy-Saving and Optimization Technology of Carbon Dioxide Captured System of Flue Gas in Coal-Fired Power*; Qingdao University of Science and Technology: Qingdao, China, 2010. (In Chinese with English abstract)